The Journal of Neuroscience, October 1993, 13(10): 4193–4213

Differential Metabolic and Electrical Activity in the Somatic Sensory Cortex of Juvenile and Adult Rats

David R. Riddle, Gabriel Gutierrez, Dake Zheng, Leonard E. White, Ann Richards, and Dale Purves

Department of Neurobiology, Duke University Medical Center, Durham, North Carolina 27710

We have examined relative levels of metabolic and electrical activity across layer IV in the primary somatic sensory cortex (S1) of the rat in relation to regions of differential postnatal cortical growth. Each of several indices used—mitochondrial enzyme histochemistry, microvessel density, Na^+/K^+ pump activity, action potential frequency, and deoxyglucose uptake—indicate regional variations of metabolic and electrical activity in this part of the brain in both juvenile (1-week-old) and adult (10–12-week-old) animals. At both ages, areas of the somatic sensory map related to special sensors such as whiskers and digital pads showed evidence of the most intense activity. Thus, mitochondrial enzyme staining, blood vessel density, and Na^+/K^+ ATPase activity were all greatest in the barrels and barrel-like structures within S1, and least in the adjacent interbarrel cortex and the cortex surrounding S1. Multiunit recordings in and around the posteromedial barrel subfield of anesthetized animals also showed that the average ratio of evoked to spontaneous activity was greater in barrels than in the surrounding, metabolically less active cortex. Furthermore, autoradiograms of labeled deoxyglucose accumulation in awake behaving animals indicated systematic differences in neural activity across S1; barrels and barrel-like structures showed more deoxyglucose accumulation than interbarrel, nonbarrel, or peri-S1 cortex. These regional differences in neural activity correspond to regional differences in neocortical growth (Riddle et al., 1992). The correlation of greater electrical activity, increased metabolism, and enhanced cortical growth during postnatal maturation suggests that neural activity foments the elaboration of circuitry in the developing brain.

[Key words: cortex, development, growth, metabolic activity, electrical activity, barrels]

We report here a series of experiments examining the relationship between regional activity and cortical growth. The effects of activity on brain development are usually considered in the context of competition and circuit segregation (e.g., Purves and Lichtman, 1985; Purves, 1988; Shatz, 1990; Goodman and Shatz, 1993). The seminal experiment that lead to this conceptual framework was carried out by D. H. Hubel and T. N. Wiesel 30 years ago (Wiesel and Hubel, 1963). They found that when one eye is closed in a kitten, a shift in ocular dominance occurs, with inputs from the deprived eye being suppressed or lost. When both eyes are closed, however, ocular dominance remains roughly normal. Evidently, the effect of monocular deprivation is generated not by the *overall* level of cortical activity, but by the *relative* activity of afferents arising from each of the two eyes. A great deal of research in developmental neurobiology has therefore been directed toward understanding the role of activity in competition. Based on Hubel and Wiesel's work, a broad consensus has emerged that the major role of activity in neural development is to "validate" and refine neural connections. Our approach in the present work has been to evaluate the relationship of electrical activity, metabolism, and brain growth per se, apart from (or in addition to) the role of activity in competition.

The primary somatic sensory cortex (S1) of juvenile and adult rats was used for these studies because of the clarity with which the somatotopic map can be seen in the cortex, and therefore measured (Fig. 1). One-week-old animals were chosen as the starting point for the study because the somatotopic map is fully formed by this age, although the cortex continues to grow substantially (Riddle et al., 1992). The constituent parts of this large region (about 15% of the neocortex in adult rats) do not grow to the same extent (Riddle et al., 1992). First, barrels and barrel-like structures in S1 grow more during postnatal maturation than the surrounding cortex. Second, barrels in regions of S1 corresponding to parts of the body that are overrepresented grow more than barrels associated with relatively underrepresented body parts. Finally, S1 as a whole grows more than the surrounding neocortex. Here we have used a variety of techniques to ask whether the metabolic and electrical activity of neocortical regions that grow more exceeds that of adjacent regions that grow less. Our results show that more active regions grow to a greater extent than less active ones, suggesting that the amount of circuitry devoted to various functions is modulated during maturation by neural activity.

Materials and Methods

All procedures were performed on male Sprague–Dawley rats obtained from Harlan Sprague–Dawley (Indianapolis, IN) and Charles River Laboratories (Raleigh, NC) at 1 week of age (juveniles) or 10–12 weeks of age (full adults). Measurements were limited to cortical layer IV in and around S1. The terms we use here to describe the features of S1 follow the conventions of our previous report (Riddle et al., 1992; see also Fig. 1). Briefly, "barrel" and "barrel-like structures" refer to the dense patches of succinate dehydrogenase (SDH) or cytochrome oxidase (CO) reaction product that are prominent in layer IV throughout S1. Within each of the five major cortical representations of the body (the repre-

Received Dec. 23, 1992; revised Mar. 18, 1993; accepted Apr. 13, 1993.

We are especially grateful to Marybeth Groelle for her unfailing assistance, and to Feri Zsuppan for help with the image analysis. We also thank Kelly Alexander for her participation in some aspects of the study. Finally, we are grateful to David Fitzpatrick, Larry Katz, Anthony LaMantia, and Peter Reinhart for helpful criticism. This work was supported by grants from the NIH and the Pew Foundation (G.G.).

Correspondence should be addressed to Dale Purves, Department of Neurobiology, Box 3209, Duke University Medical Center, Durham, NC 27710.

sentations of the whiskerpad, anterior snout, lower jaw, forepaw, and hindpaw), the regions between barrels are designated "interbarrel" cortex; "nonbarrel S1" cortex refers to barrel-free cortical regions lying within S1 but outside of the major body representations. Finally, "peri-S1" cortex refers to the neocortex immediately surrounding S1.

Mapping mitochondrial enzyme activity. Juvenile and adult rats were deeply anesthetized with sodium pentobarbital (250 mg/kg) and perfused through the heart with 0.9% saline followed by 10% glycerol for SDH histochemistry, or a solution of 3% paraformaldehyde, 0.5% glutaraldehyde, and 10% glycerol in 0.1 M sodium phosphate buffer (pH 7.4) for CO histochemistry. The cerebral cortex was removed, flattened, and frozen as previously described (Riddle et al., 1992). Serial tangential sections were cut in a cryostat (−20°C) at 25 μm, mounted onto gelatin-coated slides, and stained to demonstrate SDH activity by a modification of the method of Kugler (1982; Kugler et al., 1988). Sections were reacted at 12°C for 30 min in 7.5% polyvinyl alcohol, 50 mM sodium succinate, 10 mM sodium azide, 1 mM nitroblue tetrazolium, and 0.25 mM phenazine methosulfate in 0.1 M sodium phosphate buffer (pH 7.6). The reaction was stopped by rinsing in distilled water and fixing the sections in cold 10% formalin for 10 min. The slides were then washed in distilled water and coverslipped using Aqua-Mount (Lerner Labs, Pittsburgh, PA). For CO histochemistry, mounted sections were incubated for 90 min according to the method of Wong-Riley (1979).

The regional density of reaction product (expressed as percentage transmittance) was assessed quantitatively using a microcomputer-based image analysis system (Image 1/AT, Universal Imaging, West Chester, PA). For the sake of convenience, we use the term "activity" to describe several of our observations; we recognize that density measurements of enzyme reaction product could reflect the amount of enzyme, its specific activity, or both. For every brain, each tangential section in which barrels were apparent was digitized at a resolution of 512 × 480 using a CCD video camera; dark (no incident light) and white (empty field) images were captured and used for shading correction. This procedure reduces error due to light scattering and uneven illumination of the image plane. For analysis of mitochondrial enzyme activity, and for all other densitometric procedures (see below), the barrel borders in each section were used to create a template for measuring the staining intensity in the representations apparent in that section (Fig. 1; see also Riddle et al., 1992). The percentage transmittance of each area was determined as follows. First, in each digitized image, we drew the borders of the barrels in the five major representations and measured the percentage transmittance of each barrel. Second, we determined the density of reaction product in the interbarrel area within each representation. Third, we measured the transmittance in the nonbarrel S1 cortex, and in the peri-S1 cortex. Average values for each of these areas were coded by gray level, identified by pseudocolor, and projected onto a complete map of S1 drawn with the aid of a camera lucida. The offset of each map was adjusted to ensure that the center of the range of values was at the center of the gray scale. The contrast was inverted so that lower values of transmittance (more intense staining) appear as higher ("warmer") values on the pseudocolor scale; however, the absolute contrast of each image was not altered.

Mapping microvessel density. Following perfusion of juvenile and adult animals as described above, the descending aorta was tied off and ink (Rapidograph, Universal 3080, Bloomsbury, NJ) was injected through the cardiac cannula (8 ml for juveniles, 20 ml for adults). The cerebral cortex was then removed, flattened, and frozen (Riddle et al., 1992). Serial tangential sections were cut in a cryostat at 35 μm and processed for SDH or CO histochemistry, as described above.

Images of microvessels were made with a CCD videocamera at a final magnification of 350×, and digitized using the Image 1 analysis system. Microvessel density was defined as the area occupied by microvessel profiles per unit area of cortex (see Zheng et al., 1991). Since changing the settings of the microscope or videocamera alters the number of pixels representing blood vessels, a standard brightness and gain were used throughout these analyses. Microvessel density was measured within the barrel, interbarrel, nonbarrel S1, and peri-S1 regions in multiple 0.25 mm^2 samples (Fig. 2). For every brain studied, 5 samples from each of the five somatic representations, 10 samples from nonbarrel S1 cortex, and 11 samples from peri-S1 cortex were analyzed. To evaluate the overall distribution of blood vessels in and around S1, we used a computer-controlled automated stage to scan layer IV in 9–13 serial 35 μm sections from each brain (see Fig. 5). In this way, we determined microvessel density in approximately 1400 squares (200 × 200 μm) that covered S1 and the surrounding cortex. The values of microvessel density in each square were converted to gray levels from 1 to 255, represented with pseudocolor, and projected onto a map of S1 drawn with the aid of a camera lucida (see Fig. 5).

Mapping Na^+/K^+ ATPase activity. Juvenile and adult rats were perfused through the heart with 0.9% saline, followed by 3% paraformaldehyde, 4% sucrose in 0.1 M sodium cacodylate buffer (pH 7.4). For the juvenile animals 0.5% glutaraldehyde was added to the fixative solution to improve tissue preservation. Brains were then removed and the cortical mantles dissected and flattened. Sections were cut with a vibratome at 75 μm or with a cryostat at 50 μm, collected in cacodylate buffer, and processed by the *p*-nitrophenyl phosphate method for demonstrating Na^+/K^+ ATPase activity (Stahl and Broderson, 1976a,b). The regional density of the ATPase reaction product was assessed in the same manner as the reaction products of SDH and CO (see above). In order to evaluate the specificity of the technique, ouabain (Sigma, St. Louis, MO), an inhibitor of Na^+/K^+ ATPase, was added to the preincubation and incubation media in control trials. Incubation in 30 mM ouabain abolished the specific staining of barrel, interbarrel, and nonbarrel regions.

Mapping electrical activity. Juvenile and adult rats were anesthetized for electrophysiological recording with urethane (1.5 gm/kg, i.p.) and placed in a stereotaxic apparatus or head-holder that allowed electrodes to be positioned perpendicular to any region of the cortical surface. Rectal temperature was maintained at 37°C by means of an automatic temperature control system. The skull was exposed through a midline incision, the temporalis muscle partially reflected, and a craniotomy opened over the left posteromedial barrel subfield (PMBSF). We focused on this region because of its well-established relationship to specific peripheral sensors (Woolsey and Van der Loos, 1970) and the relatively large amount of interbarrel cortex. The dura was removed to facilitate penetration of the microelectrodes, and the surface of the brain covered with 2% agar to prevent drying.

Multiunit activity was recorded with tungsten microelectrodes (impedances, 0.3–2.0 MΩ; Frederick Haer and Co., Brunswick, ME) in and around the PMBSF. The electrode signal was amplified, band pass filtered (500–10,000 Hz), and monitored on an oscilloscope and loudspeaker. Spike frequency was analyzed on line using a slope/height window discriminator and a timed counter. The window discriminator was adjusted by first measuring the peak-to-peak noise amplitude (10–20 μV) with the electrode tip immersed in the agar covering the brain; the threshold of the window discriminator was then set at 1.5 times the noise amplitude. The electrode tip was advanced to 500–600 μm in juveniles and 650–750 μm in adults, depths empirically determined to be mid-layer IV. A 10 min period was allowed to pass before beginning data collection.

At each recording site, the total number of action potentials occurring in consecutive 10 sec samples was determined during alternating periods of rest and peripheral stimulation. Thus, in the first 10 sec sample basal activity was recorded in the absence of peripheral stimulation; a second 10 sec sample was then obtained during stimulation by passing a hand-held stream of air over the contralateral face in a rapid circular motion. This procedure deflected all of the whiskers (and common fur) in a variety of directions, an important consideration since individual units in the PMBSF are often directionally selective (Simons, 1978). In addition to stimulating vibrissal receptors, this method presumably acti-

→

Figure 1. Histochemical demonstration of primary somatic sensory cortex in the rat, and definition of its constituent parts. *A*, Digitized image of a single SDH-stained tangential section of the primary somatic sensory cortex in a juvenile (1-week-old) rat. Scale bar, 2 mm. *B*, Complete S1 map in the same animal reconstructed from multiple sections. Barrels (*gray*), interbarrel areas (*yellow*), and nonbarrel S1 areas (*red*) in each section were defined using the centroids of the outermost barrels in each major representation (see Riddle et al., 1992, for details). Barrels related to facial whiskers around the naris and eye, near the corner of the mouth, and at the midline neck (all coded *black*) were omitted from the analysis, and consequently are not shown in subsequent maps. Similarly, the trunk representation with its less distinct borders was not included in most analyses, and is also not shown in subsequent figures.

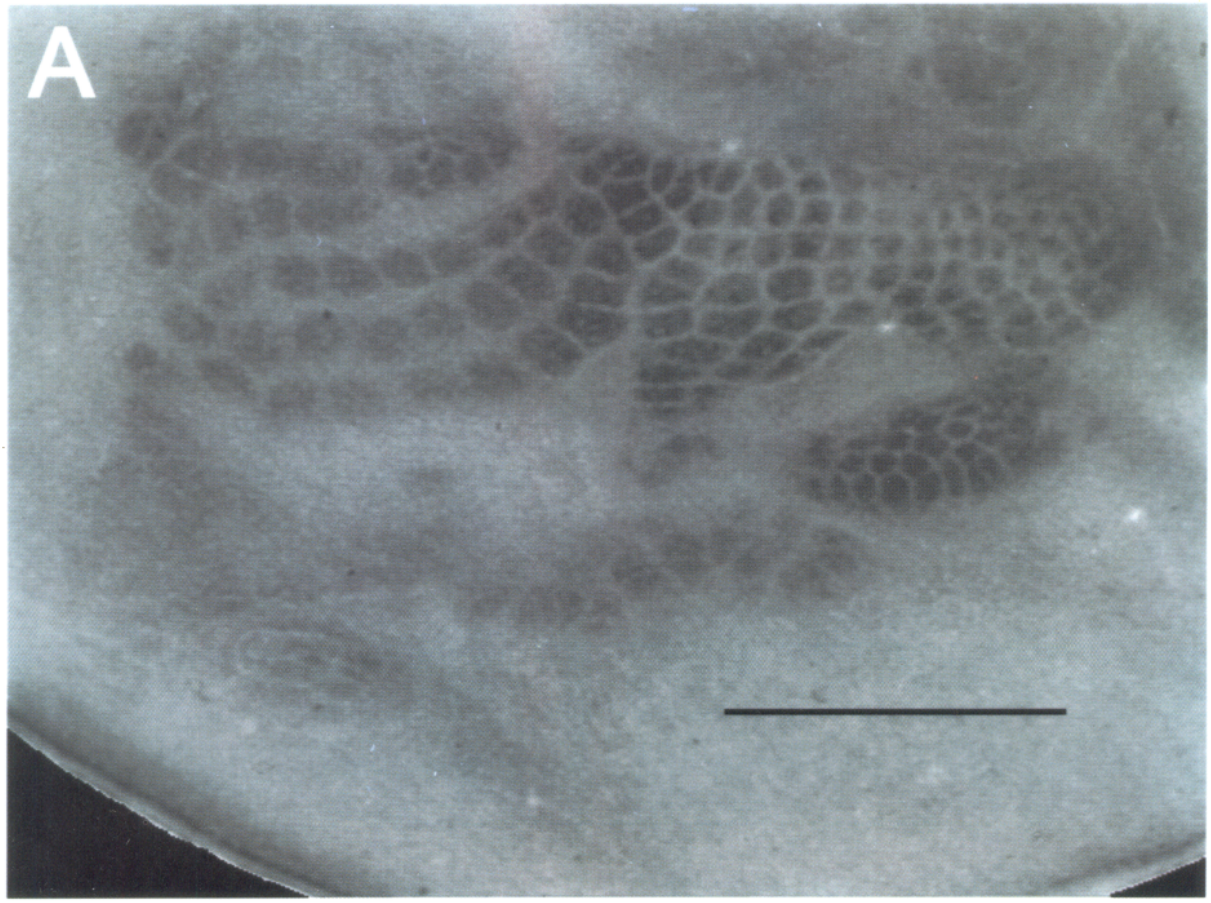
A

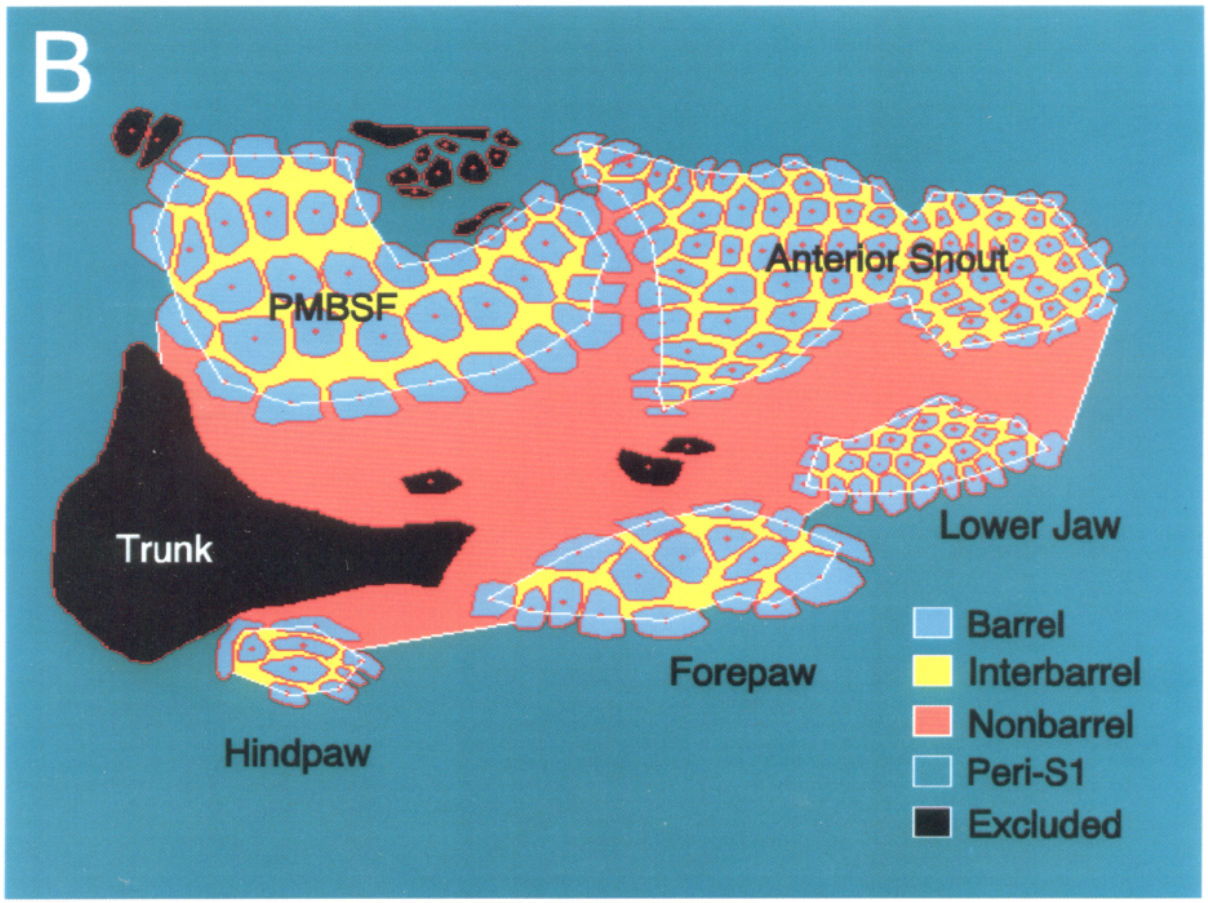
B
PMBSF
Anterior Snout
Trunk
Lower Jaw
Forepaw
Hindpaw
Barrel
Interbarrel
Nonbarrel
Peri-S1
Excluded

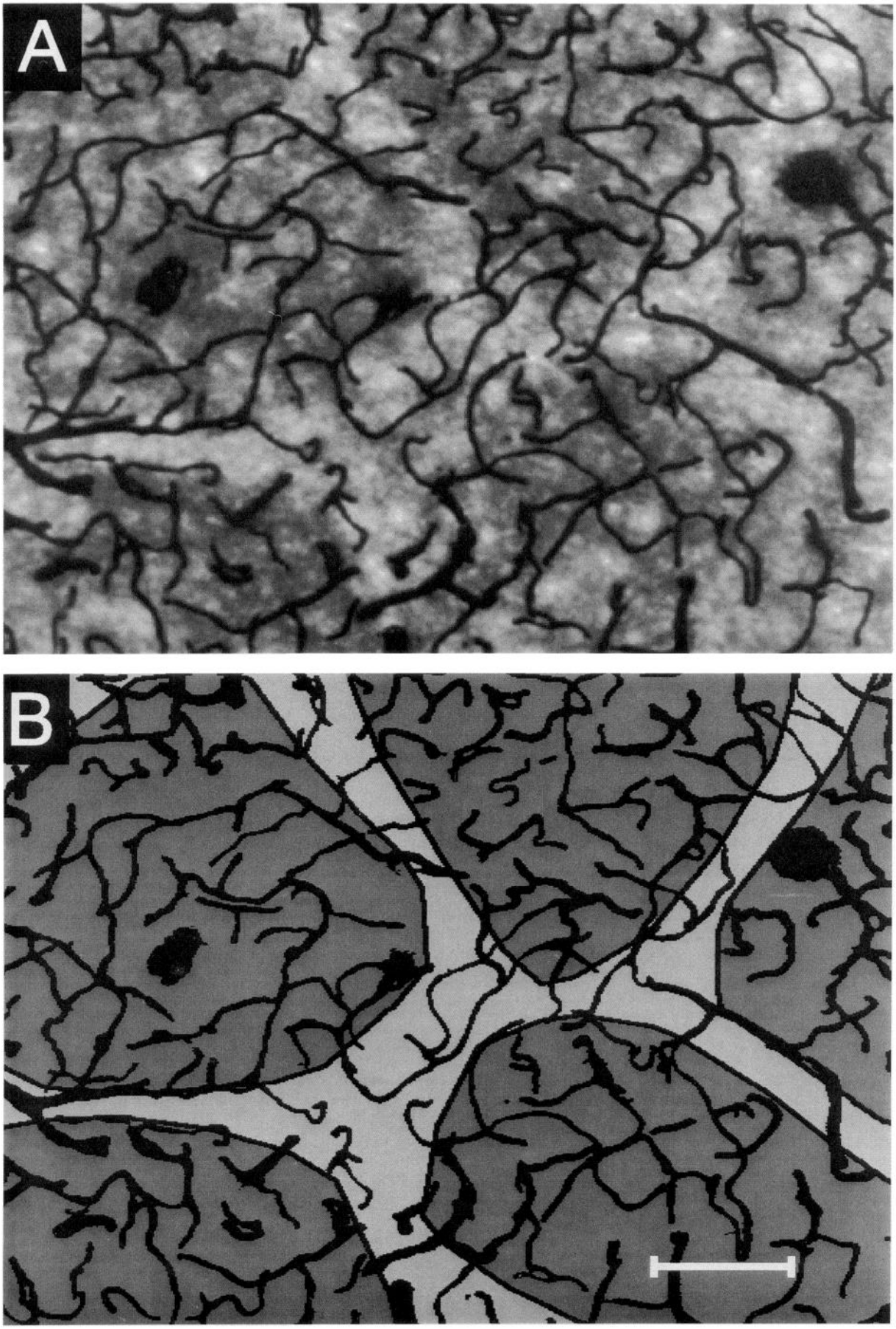
A
B

vated a variety of other cutaneous mechanoreceptors. The next 10 sec sample was again of basal activity, and so on for the full run of 10 samples. After a 5 min waiting period, another set of 10 alternating samples was obtained to allow for possible fluctuations in arousal or other systemic changes that might affect basal or evoked cortical activity. Finally, the position of the electrode tip was marked by a small electrolytic lesion (3 μA for 3 sec). Typically, 6–10 electrode penetrations were made in each animal. After the experimental session was complete, the animal was perfused and the brain processed for SDH histochemistry, as described above. Each electrolytic lesion was localized both vertically and horizontally with respect to the pattern of barrels.

For each recording site, we calculated the mean number of spikes in the basal samples and in the samples obtained during peripheral stimulation. Two aspects of these data were evaluated: (1) the level of basal activity and (2) the ratio of evoked to basal activity. All measurements were grouped into barrel, interbarrel, and nonbarrel S1 categories according to the location of the electrolytic lesions.

Mapping ^{3}H-2-deoxyglucose uptake. Tritiated deoxyglucose (2-DG) was infused in awake behaving juvenile and adult animals. In juvenile rats, infusions of 2-DG were made in the jugular vein after exposure of the vessel under local anesthesia (lidocaine, 10 mg/ml). This procedure took no more than 5 min. Adult rats were anesthetized with a mixture of ketamine and xylazine (40 and 2 mg/kg, i.m., respectively) and a polyethylene catheter was implanted into the femoral vein. The adult animals were allowed to recover from anesthesia for 10–12 hr before isotope injection. For both juveniles and adults, a solution of ^{3}H-2-deoxyglucose (American Radiolabeled Chemicals, St. Louis, MO) in 0.9% saline (3 μCi/gm body weight) was introduced over 15 sec. The infusions were always made at the same time of day to avoid any metabolic effects of diurnal rhythms (Richardson and Rosen, 1971). After 45–50 min, the rats were deeply anesthetized with pentobarbital (250 mg/kg, i.p.) and decapitated. The brains were rapidly removed, hemisected, flattened, and frozen. To evaluate the importance of normal mechanoreceptor activity and wakefulness to 2-DG labeling under these conditions, similar experiments were performed on adult animals fully anesthetized with sodium pentobarbital (50 mg/kg, i.p.) or urethane (1.5 gm/kg, i.p.) during the 45 min period of isotope uptake. Serial tangential sections were cut in a cryostat (−25°C) at 20 μm, thaw-mounted onto gelatin-coated coverslips, and quickly dried on a hot plate (50°C). The coverslips were overlaid with tritium-sensitive Hyperfilm (Amersham, Arlington Heights, IL) and exposed for 10–15 d at 4°C. The film was developed in Kodak D-19 for 5 min, fixed with Kodak rapid-fixer for 5 min, washed in running water for 15 min, and air dried. The tissue sections were then processed for SDH histochemistry, as described above.

The autoradiograms were analyzed by quantitative densitometry after superimposing them onto the corresponding SDH-stained sections. To assure correct alignment of the images, fiducial marks were made prior to exposure. Detailed measurements of transmittance in barrel, interbarrel, and nonbarrel regions were made after defining individual barrels, as described above; comparisons were carried out by averaging the transmittance values of each region. The average values of transmittance were coded as gray scale values and plotted on the complete digitized map of S1 (see Fig. 12).

Regional densitometric comparisons. Densitometric analyses of mitochondrial enzyme activity, Na^+/K^+ ATPase activity, and 2-DG uptake were carried out in a similar fashion. For each relevant section, a series of comparisons were performed to evaluate the relative transmittance in the pertinent regions in and around S1. These comparisons were expressed as the percentage difference in staining intensity in one region (e.g., barrels) relative to the staining intensity in another region of the same section (e.g., interbarrel or nonbarrel S1 cortex). The corresponding values across different sections from the same brain were then averaged, and group means for juvenile and adult populations determined.

Results

Differential growth of the primary somatic sensory cortex

In an earlier article (Riddle et al., 1992), we described the areal growth of the primary somatic sensory cortex and its constituent parts in the developing rat. Our major findings were that (1) as a group, barrels and barrel-like structures grow more than other regions of S1; (2) barrels in the representation of the head grow substantially more during maturation than those in the representations of the paws; and (3) the primary somatic sensory cortex as a whole grows more than the surrounding neocortex. These points are summarized in Figure 3. By each of the parameters examined in the present report—mitochondrial enzyme activity, microvessel density, sodium-potassium pump activity, action potential frequency, and 2-DG uptake—the regions of greatest neural activity correspond to the regions of greatest growth.

Table 1. Relative levels of SDH activity in the rat somatic sensory cortex

Subjects	Number of hemispheres examined	Percentage differences (mean ± SEM) Barrel: interbarrel cortex	Barrel: nonbarrel S1 cortex	Barrel: peri-S1 cortex
Juvenile animals (1 week old)	5	17 ± 2	33 ± 4	28 ± 3
Adult animals (10–12 weeks old)	4	13 ± 5	16 ± 5	16 ± 7

Ratios for each of the three percentage difference categories were always determined in individual sections to compensate for any differences in staining; percent differences were calculated as the barrel value minus the comparative value, divided by the comparative value.

Distribution of mitochondrial enzyme activity

The intensity of SDH activity across S1 in five juvenile hemispheres (four rats) was measured by determining the relative density of reaction product in barrel, interbarrel, nonbarrel S1, and peri-S1 regions. Barrels stained more intensely than interbarrel, nonbarrel, or peri-S1 cortex (Table 1, Fig. 4*A*). Moreover, barrels in the head representations stained more intensely than barrels in the paw representations (Fig. 4*A*), and S1 as a whole (the combined barrel, interbarrel, and nonbarrel S1 regions) exhibited greater SDH activity than the peri-S1 cortex (a 15 ± 1% difference). Thus, the pattern of enzyme activity in juvenile animals closely parallels the pattern of differential growth (compare Figs. 3, 4*A*).

The pattern of SDH activity in four adult hemispheres (four rats) was similar to that in juvenile animals, although the regional differences in staining were less pronounced (Table 1, Fig. 4*B*). In addition, three juvenile and three adult hemispheres were processed for CO histochemistry. As expected for another mitochondrial enzyme involved in oxidative metabolism, the pattern of CO staining was similar to that of SDH.

Distribution of microvessels

To obtain a different index of regional cortical metabolism, we measured the vascularization of layer IV after perfusion with ink. An analysis of microvessel distribution in barrel, interbarrel, nonbarrel, and peri-S1 cortex in 10 juvenile hemispheres

←

Figure 2. Analysis of microvessel distribution in and around the primary somatic sensory cortex. *A*, Photomicrograph of ink-filled microvessels and barrels (revealed by CO staining) in the anterior snout representation. *B*, Digitized and processed image of microvessel profiles in *A*; *lines* were drawn to indicate barrel borders. Such images were used to measure microvessel density in the various regions of S1. Scale bar, 100 μm.

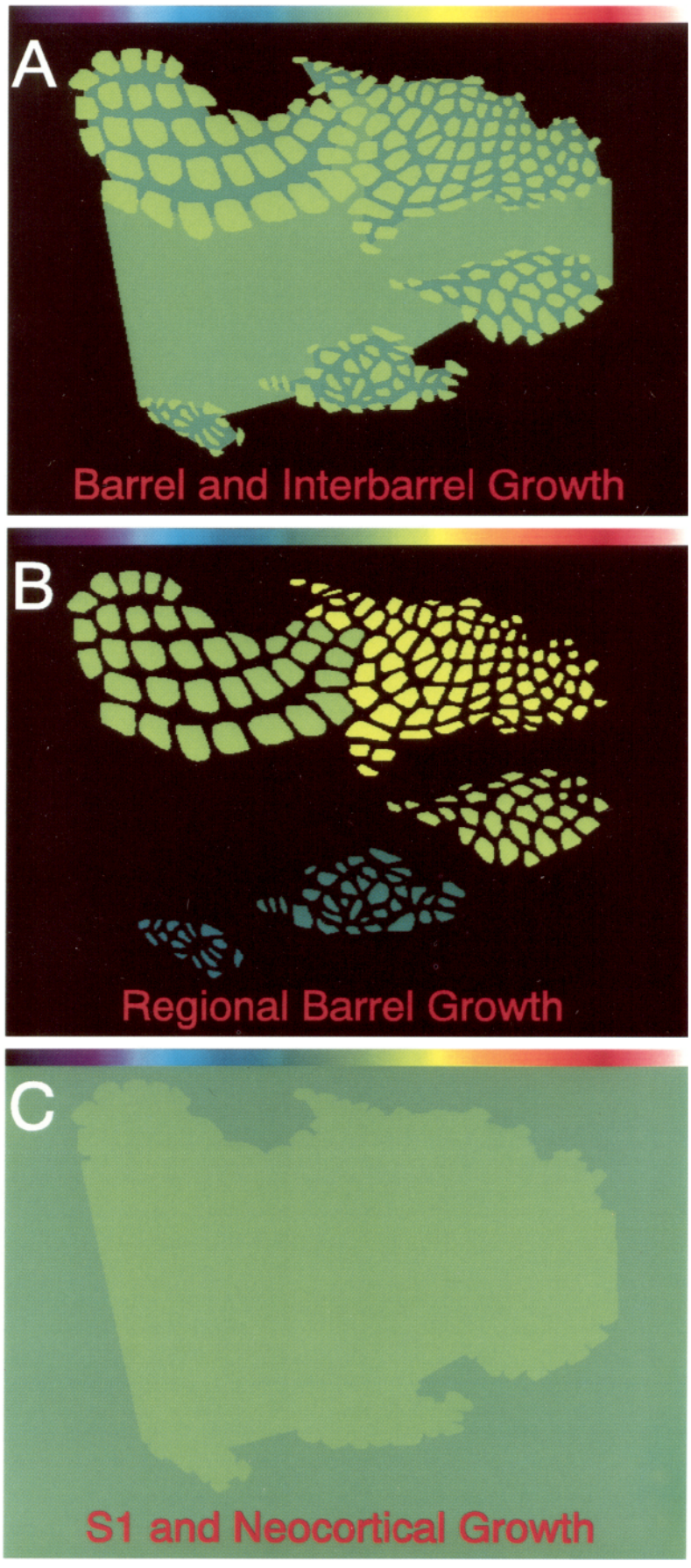

Figure 3. Differential pattern of postnatal growth in the primary somatic sensory cortex. The average amount of postnatal growth (indicated as the percentage increase in area from 1 to 10 weeks of age) is color coded for each region; *warmer colors* indicate the greater growth. Barrels grow more than other areas in S1 (*A*), barrels in the head representations grow more than those in the paw representations (*B*), and S1 as a whole grows more than the surrounding cortex (*C*). The pattern of differential growth should be compared with the patterns of differential metabolic and electrical activity presented in subsequent figures (based on data in Riddle et al., 1992).

Table 2. Microvessel distribution in layer IV of the rat somatic sensory cortex

Hemisphere number	Mean blood vessel density (expressed as percentage of sampling area)				Percentage differences		
	Barrel cortex	Interbarrel cortex	Nonbarrel S1 cortex	Peri-S1 cortex	Barrel: interbarrel cortex	Barrel: nonbarrel S1 cortex	Barrel: peri-S1 cortex
Juvenile animals (1 week old)							
1	11.0	5.2	7.9	7.0	112	39	57
2	9.5	4.4	8.0	6.9	116	19	38
3	8.7	3.9	6.9	6.6	123	26	32
4	9.7	4.6	6.3	6.4	111	54	52
5	9.7	4.9	6.6	6.4	98	47	52
6	8.0	3.8	5.6	5.1	111	43	57
7	7.8	3.1	4.3	4.3	152	81	81
8	8.4	4.0	6.6	6.3	110	27	33
9	9.1	4.6	6.0	6.0	98	52	52
10	8.8	3.5	6.0	5.3	151	47	66
Mean ± SEM	9.1 ± 0.3	4.2 ± 0.2	6.4 ± 0.3	6.0 ± 0.3	118 ± 6	43 ± 6	52 ± 6
Adult animals (10–12 weeks old)							
1	10.2	6.8	8.6	7.4	50	19	38
2	18.2	13.7	15.8	14.1	33	15	29
3	13.0	9.2	11.3	9.4	41	15	38
4	13.5	9.4	11.9	10.3	44	13	31
5	15.9	11.3	14.3	13.4	41	11	19
6	18.2	11.8	15.6	14.8	54	17	23
7	16.6	9.7	13.3	13.7	71	25	21
8	16.1	10.9	12.3	11.1	48	31	45
9	16.9	11.3	13.6	13.7	50	24	23
10	14.6	9.6	11.8	11.0	52	24	33
Mean ± SEM	15.3 ± 0.8	10.4 ± 0.6	12.9 ± 0.7	11.9 ± 0.8	48 ± 3	19 ± 2	30 ± 3

(seven animals) showed that microvessel density was always greater within barrels than in other regions (Table 2). Furthermore, the average microvessel density in barrels varied among representations. For example, the average density of vessels in barrels of the anterior snout representation was 27% greater than that in the barrels of the hindpaw representation.

A more general analysis of microvessel density in layer IV of the parietal and frontal cortex was undertaken in three additional hemispheres from three juvenile rats by automated scanning (see Materials and Methods). These measurements showed that the average vascular density in each of the five major representations within S1 is higher than in the nonbarrel region, and that the head representation is more heavily vascularized than the paw regions (Fig. 5). In addition, S1 as a whole stands out from the surrounding neocortex as a region of generally greater vascular density.

We also analyzed microvessel density in 13 hemispheres from 11 adult animals (10 hemispheres for regional sampling, 3 for automated scanning). Although the differences were less pronounced, the pattern of microvessel distribution was similar to

→

Figure 4. Distribution of SDH activity in layer IV of the primary somatic sensory cortex of a representative juvenile (*A*) and adult (*B*) rat. Average values for each region were coded by gray level and projected onto a map of S1 reconstructed from multiple sections with the aid of a camera lucida. More intense staining appears as higher (warmer) values on the pseudocolor scale. Scale bar, 2 mm.

Figure 5. Distribution of microvessel density in layer IV of the primary somatic sensory cortex of a representative juvenile rat. *A*, Overall map of microvessel distribution. Microvessel density was analyzed sequentially in 200 × 200 μm squares, converted to gray levels from 1 to 255, color coded, and then projected onto a map of the S1 barrels reconstructed from the same sections. Note that measurements distant from S1 are less confidently assigned to layer IV than measurements within and immediately around S1. *B*, The average microvessel density in the major somatic representations within S1 is higher than both the nonbarrel S1 regions and the peri-S1 cortex. Scale bar, 2 mm.

Figure 6. Distribution of microvessel density in layer IV of the primary somatic sensory cortex of a representative adult rat. *A*, Overall map of microvessel distribution in layer IV of S1. Microvessel density was analyzed in the same fashion as in juvenile animals. *B*, Although the differences are less pronounced than in juveniles (compare Fig. 5), the average density in each of the major somatic representations within S1 is higher than in the nonbarrel S1 regions and the cortex surrounding S1. Scale bar, 2 mm.

Figure 7. Distribution of Na^+/K^+ ATPase activity in the primary somatic sensory cortex of a representative juvenile rat. *A*, Montage of digital images showing characteristic distribution of the Na^+/K^+ ATPase activity in layer IV of S1 and the surrounding cortex. *B*, The average values for each region were coded by gray level and projected onto a map of S1 reconstructed from multiple sections with the aid of a camera lucida. Scale bar, 2 mm.

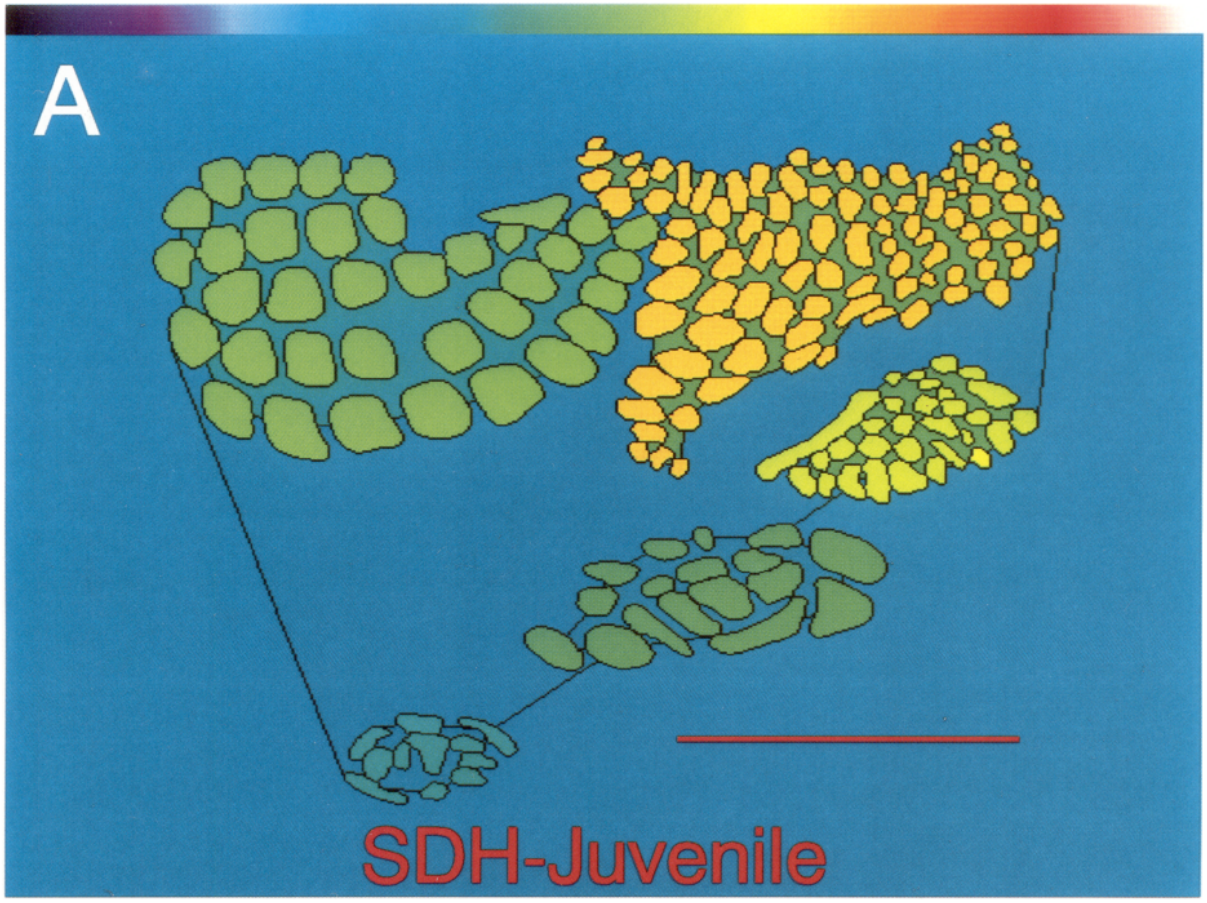
A
SDH-Juvenile

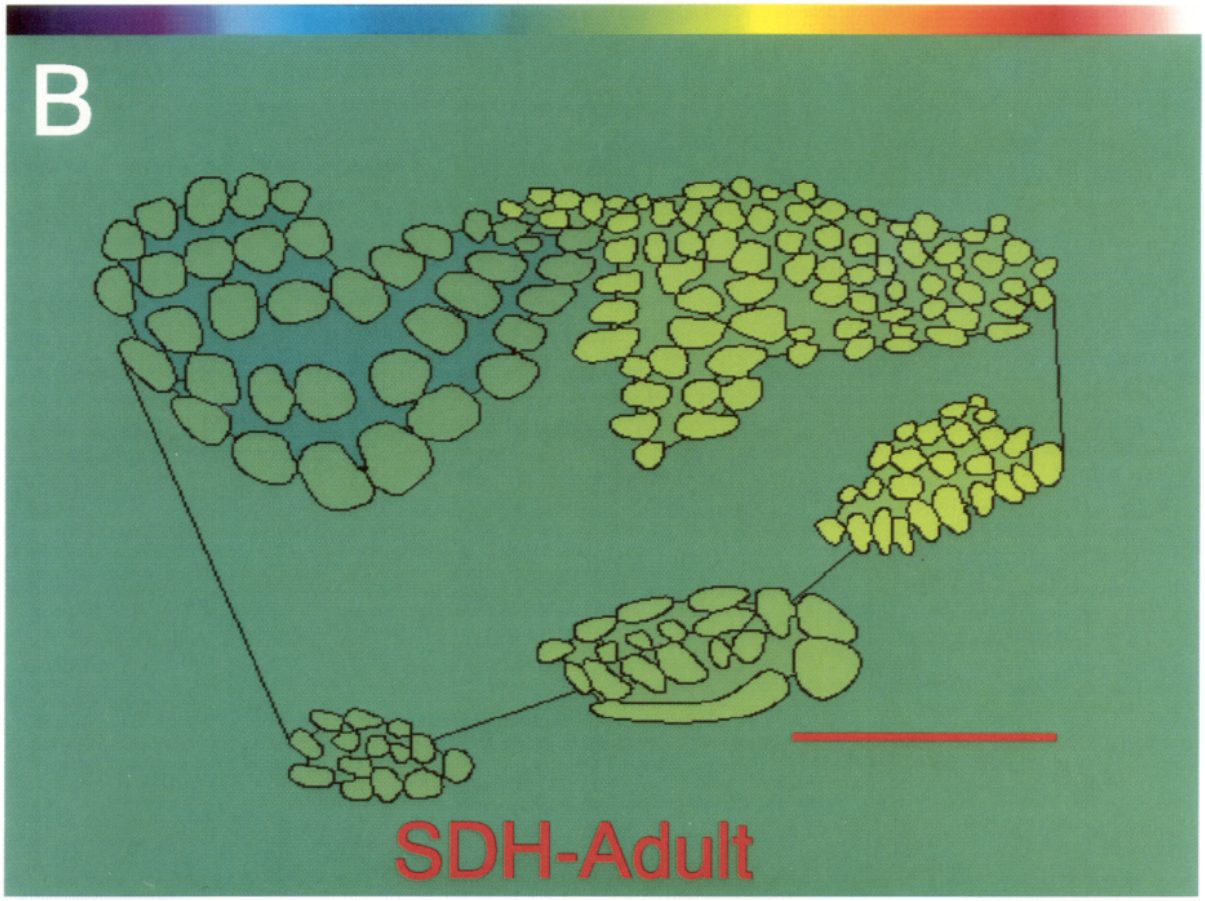
B
SDH-Adult

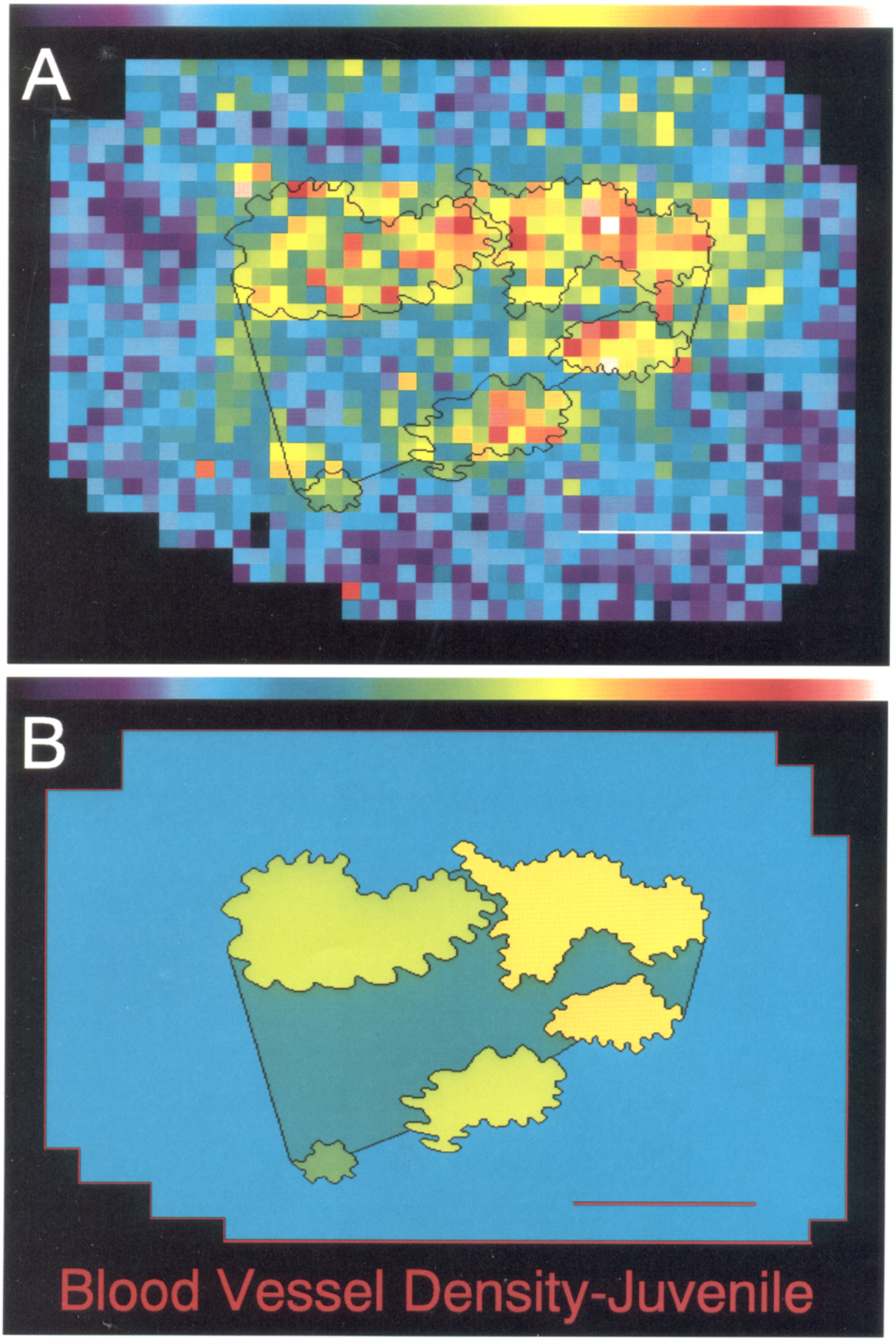
A
B
Blood Vessel Density-Juvenile

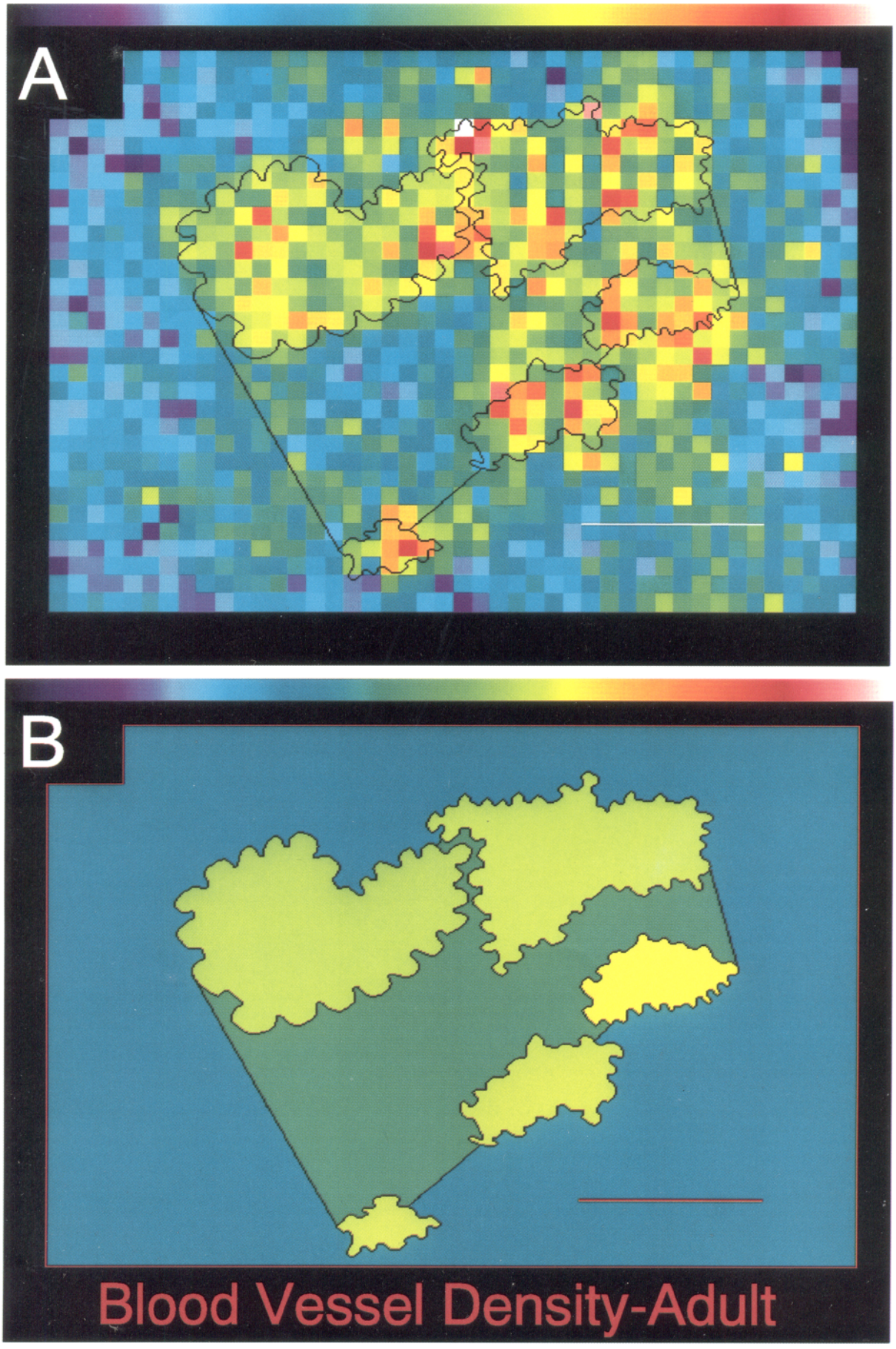
A
B
Blood Vessel Density-Adult

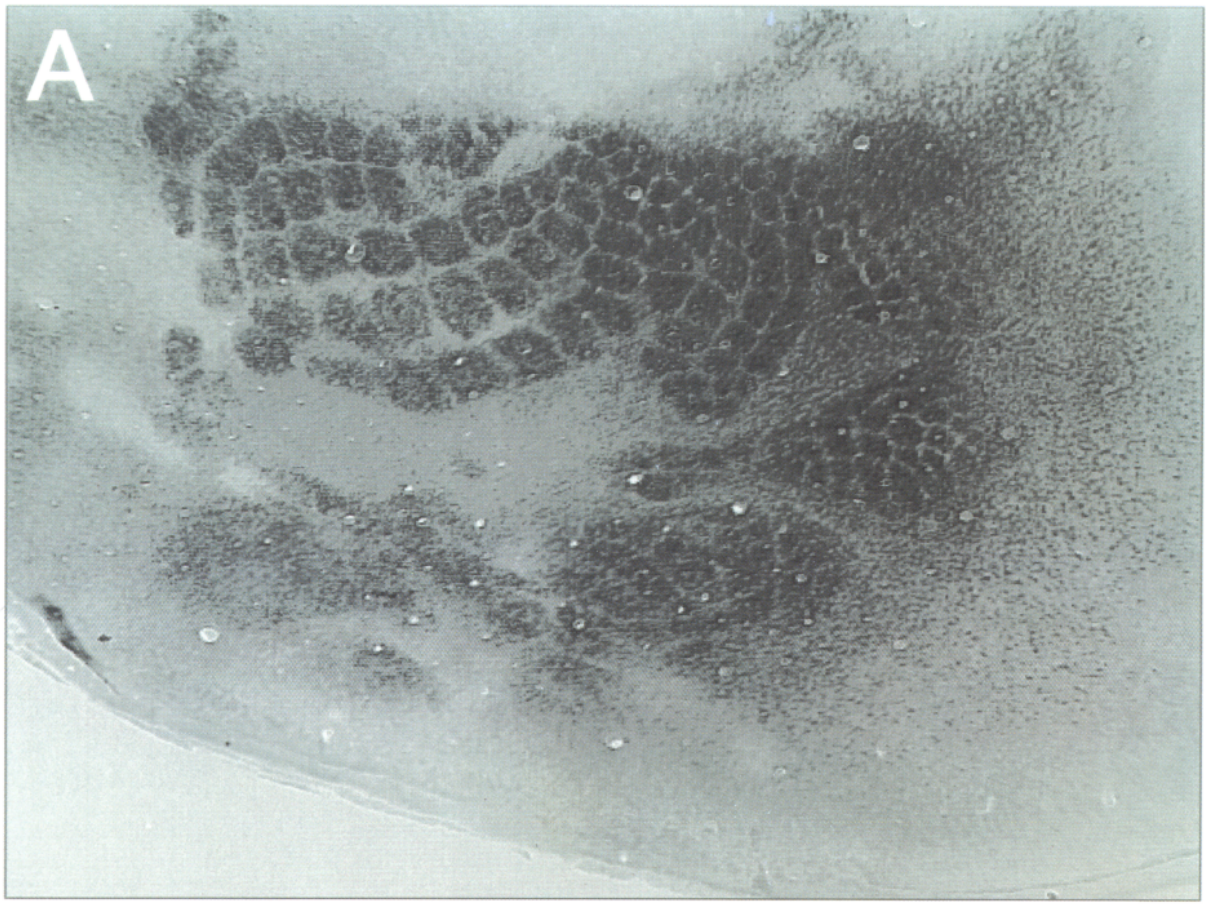
A

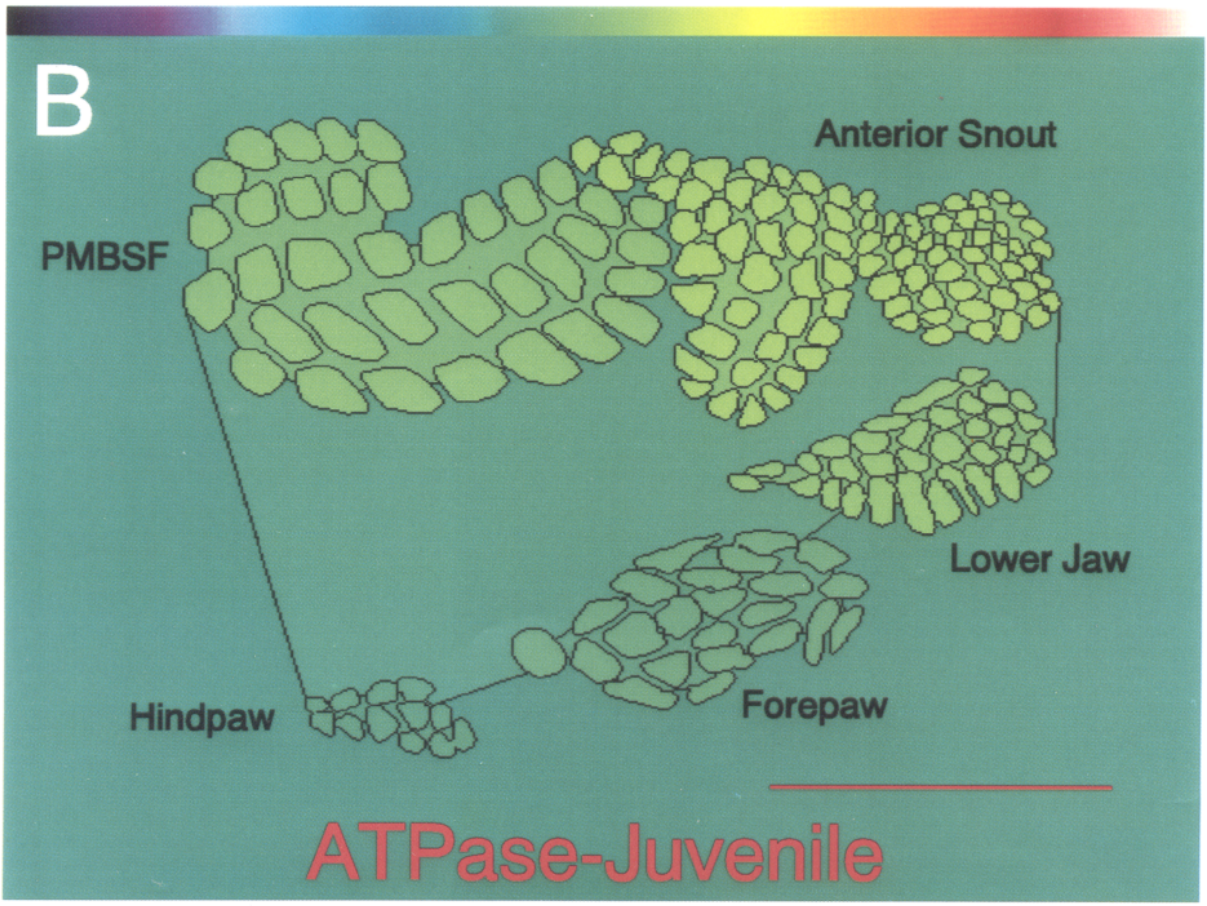
B
Anterior Snout
PMBSF
Lower Jaw
Hindpaw
Forepaw
ATPase-Juvenile

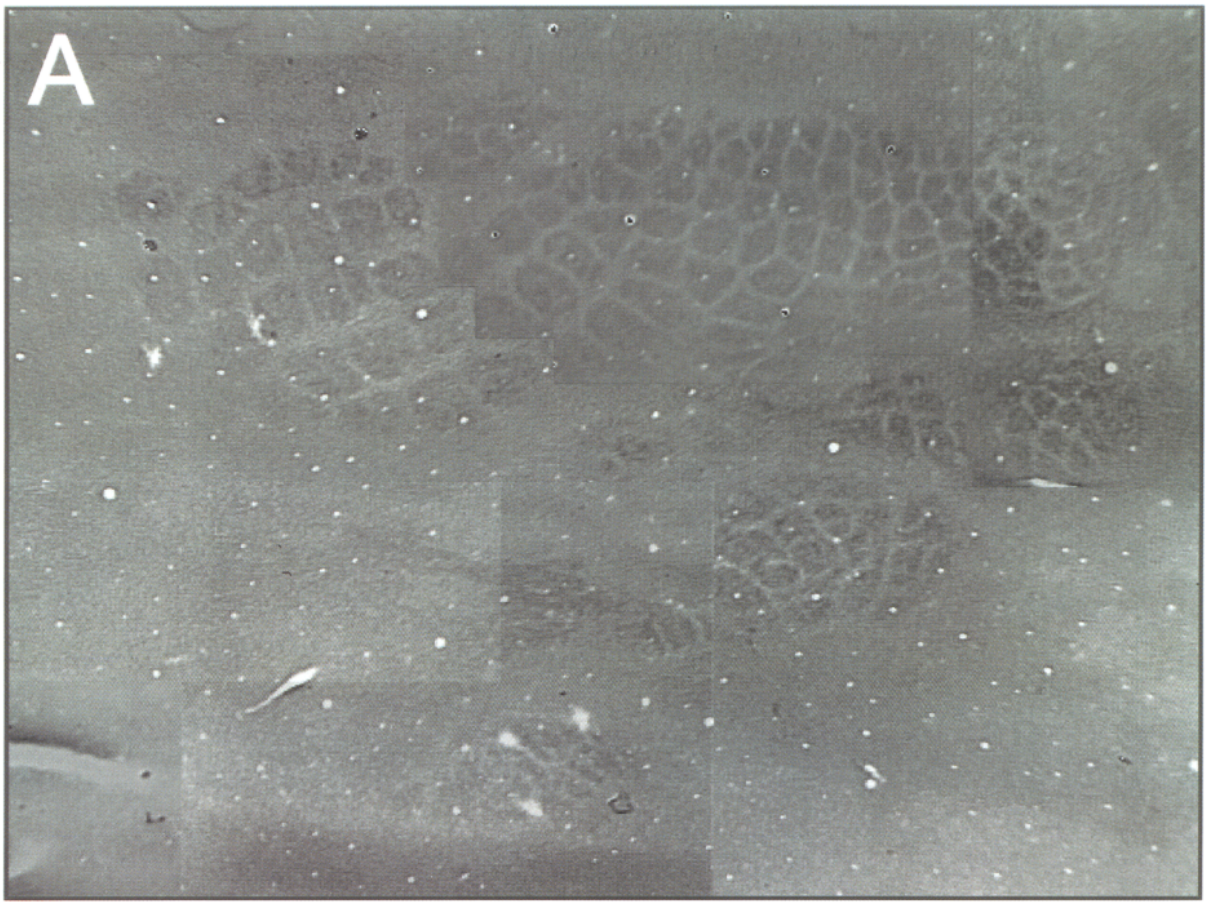
A

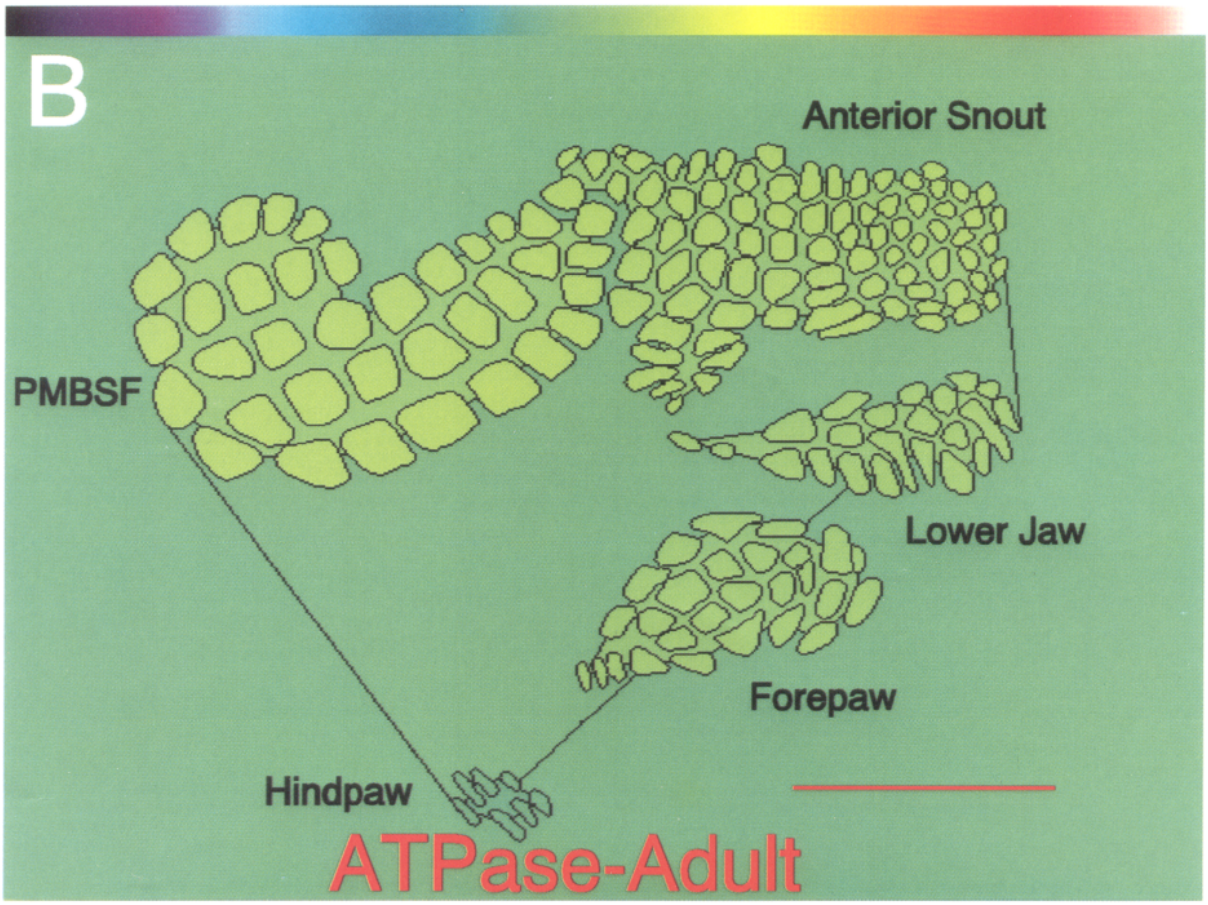
B
Anterior Snout
PMBSF
Lower Jaw
Forepaw
Hindpaw
ATPase-Adult

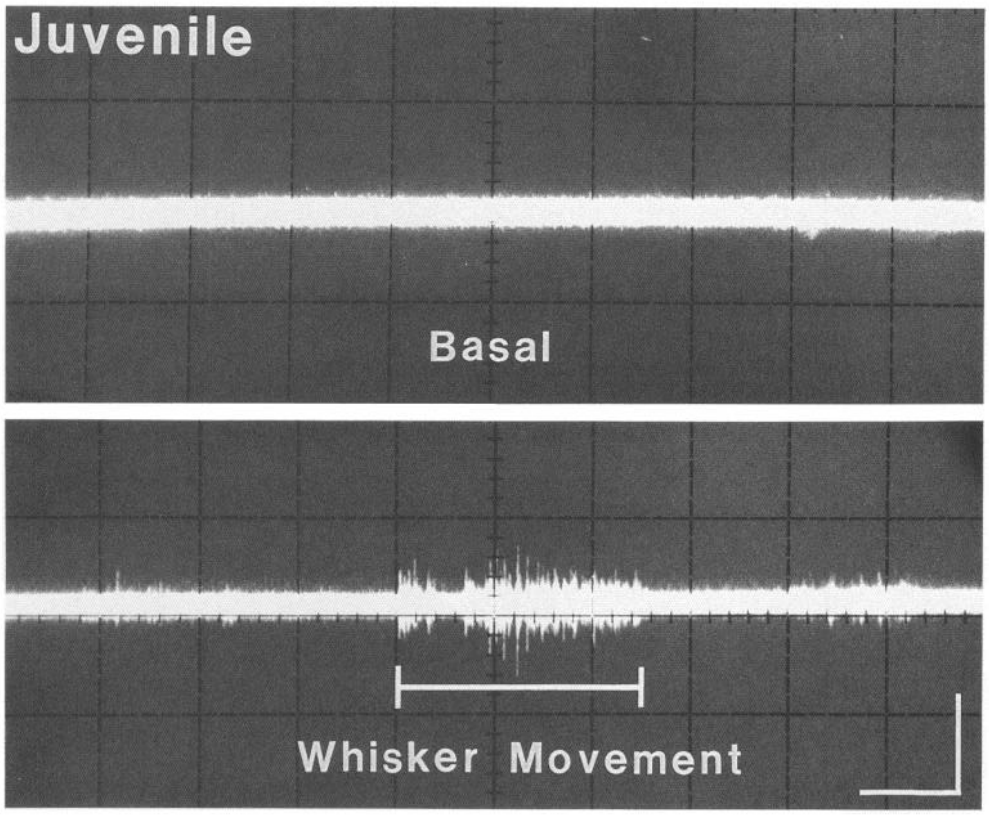

Figure 9. Multiunit activity in layer IV of the primary somatic sensory cortex of a urethane-anesthetized juvenile rat. Each panel shows a single trace from the same recording site within the C2 barrel. *Upper panel*, No action potentials were observed under basal conditions. *Lower panel*, When the C2 whisker was moved (*bracket*), evoked activity was readily apparent. Calibration: 0.5 sec, 100 μV.

that in juveniles (Table 2, Fig. 6). Thus, the distribution of microvessels in layer IV of S1 in both juvenile and adult animals corresponds to the pattern of mitochondrial enzyme staining, and to the pattern of differential cortical growth (see Fig. 3).

Distribution of sodium/potassium ATPase activity

In four juvenile hemispheres (three rats), barrels showed greater ATPase activity than the interbarrel, nonbarrel, or peri-S1 cortex (Table 3). Differences in barrel ATPase activity among the representations within S1 were also apparent (Fig. 7). Thus, barrels stained more intensely in the head representation than in the paw representations. As was the case for patterns of mitochondrial enzyme staining and blood vessel density, S1 as a whole exhibited greater ATPase activity than the surrounding cortex.

The same pattern of Na^+/K^+ ATPase activity was observed in four adult hemispheres (three rats) (Table 3, Fig. 8). As with the other measures we used, the regional differences in ATPase activity were present but somewhat less prominent than in juvenile animals.

Regional differences in ongoing electrical activity

The pattern of ATPase activity described in the preceding section suggests that ongoing levels of neural signaling vary across S1 (see Discussion). To substantiate this implication, we examined multiunit activity in the PMBSF and in the nonbarrel S1 cortex immediately adjacent to the E row of barrels in anesthetized animals. Units in interbarrel and nonbarrel cortex in and around the PMBSF often respond to mechanosensory stimulation of the face (Welker, 1976; Chapin and Lin, 1984). In accord with previous observations (Armstrong-James, 1975; Armstrong-James et al., 1985), we found very little spontaneous activity in S1 in six juvenile animals (Fig. 9, upper panel). We could, however, evoke electrical activity for recording sites near barrel centers by moving the corresponding whisker (Fig. 9, lower panel). Although the small size of the evoked responses

Table 3. Relative levels of Na^+/K^+ ATPase activity in the rat somatic sensory cortex

Subjects	Number of hemispheres examined	Percentage differences (mean ± SEM)		
		Barrel: interbarrel cortex	Barrel: nonbarrel S1 cortex	Barrel: peri-S1 cortex
Juvenile animals (1 week old)	4	18 ± 1	29 ± 1	35 ± 1
Adult animals (10–12 weeks old)	4	15 ± 3	19 ± 2	20 ± 3

Values were calculated as in Table 1.

←

Figure 8. Distribution of Na^+/K^+ ATPase activity in the primary somatic sensory cortex of a representative adult rat. *A*, Montage of digital images showing characteristic distribution of the Na^+/K^+ ATPase activity in layer IV of S1 and the surrounding cortex. *B*, Although the variations in ATPase activity are less striking than in juvenile animals (compare Fig. 7), the average density in barrels remains generally higher than in the interbarrel, nonbarrel S1, and peri-S1 regions. Scale bar, 2 mm.

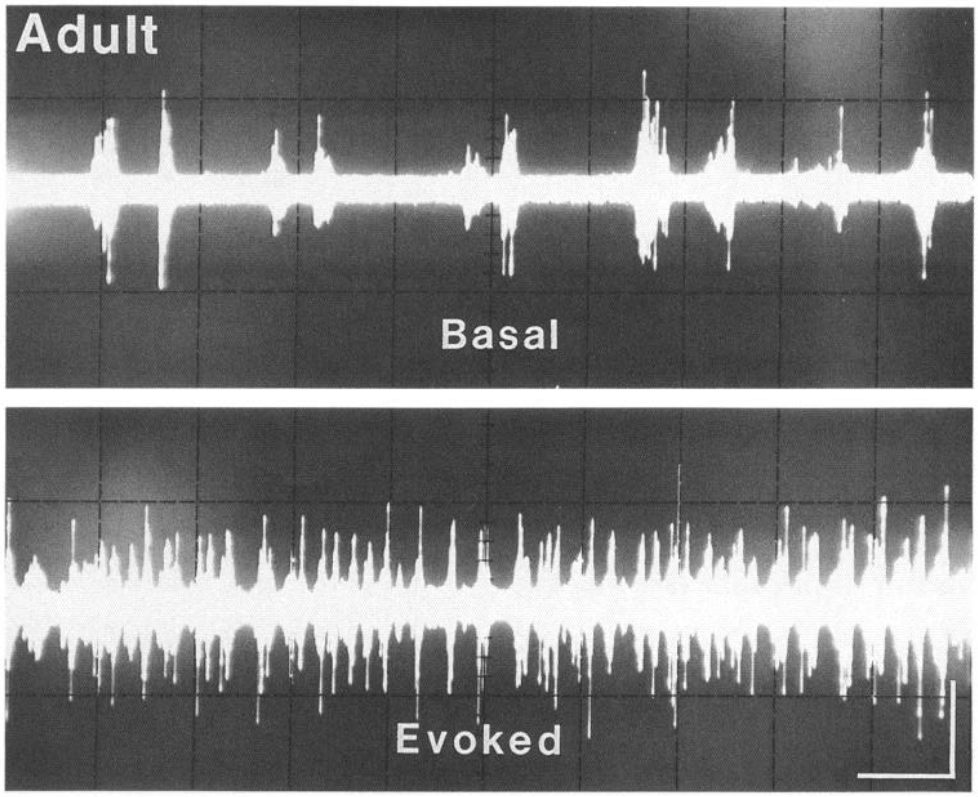

Figure 10. Multiunit activity in layer IV of the primary somatic sensory cortex of a urethane-anesthetized adult rat. Each panel shows a single trace recorded from the same site within the D3 barrel. *Upper panel*, Under basal conditions, multiunit activity occurred in characteristic bursts. *Lower panel*, When whiskers (and other mechanoreceptors) were continuously stimulated by passing a stream of air over the face, a large and sustained increase in electrical activity was observed. Calibration: 0.5 sec, 100 μV.

precluded the quantitative analysis of unitary activity carried out in mature animals (see below), these observations show that stimulation of peripheral mechanoreceptors evokes electrical activity in barrels at least as early as 1 week of age.

We next examined electrical activity in and around the PMBSF in 33 adult animals (Fig. 10). First, we analyzed basal activity (i.e., the number of action potentials recorded per unit time in the absence of peripheral stimulation) within and around this region of the S1 map. As reported previously (Armstrong-James and Fox, 1983; Armstrong-James et al., 1985; Fox and Armstrong-James, 1986), basal activity recorded from adult rats anesthetized with urethane consists mainly of prominent bursting activity in the delta range (<4 Hz) throughout S1 and the surrounding neocortex (Fig. 10, upper panel). Such basal activity was greater within the PMBSF than in the nonbarrel S1 cortex (Table 4).

We then compared levels of basal electrical activity to levels obtained at the same recording site during sustained stimulation of the mystacial vibrissae and surrounding regions of the face and snout (Figs. 10, 11) (see Materials and Methods). In 89 such

Table 4. Electrophysiological measurements of multiunit activity recorded within and around the PMBSF

Measure	Barrel cortex	Interbarrel cortex	Nonbarrel S1 cortex[a]
Basal activity[b]	107.7 ± 15.7 (n = 13)	110.8 ± 19.5 (n = 13)	45.8 ± 7.4[c] (n = 13)
Net increase in activity with peripheral stimulation[d]	457.9 ± 124.8 (n = 10)	154.4 ± 28.6[e] (n = 10)	57.4 ± 18.5[e,f] (n = 10)
Ratio of evoked to basal activity[g]	5.9 ± 1.3 (n = 10)	3.5 ± 0.9[e] (n = 10)	2.2 ± 0.4[e] (n = 10)

[a] Within 0.5 mm of the E row of barrels.

[b] Counts of action potentials per 10 sec interval in the absence of peripheral stimulation (mean ± SEM; n = number of animals).

[c] Value significantly less than the corresponding value for the barrel and interbarrel groups ($p < 0.005$, nonparametric ANOVA for multiple comparisons).

[d] Difference between counts obtained during sustained peripheral stimulation and counts obtained under basal conditions; values were determined for each recording site individually (mean ± SEM; n = number of animals).

[e] Value significantly less than the corresponding value for the barrel group ($p < 0.005$).

[f] Value significantly less than the corresponding value for the interbarrel group ($p < 0.005$).

[g] Ratios of counts obtained during sustained peripheral stimulation to counts obtained under basal conditions; values were determined for each recording site individually (mean ± SEM; n = number of animals).

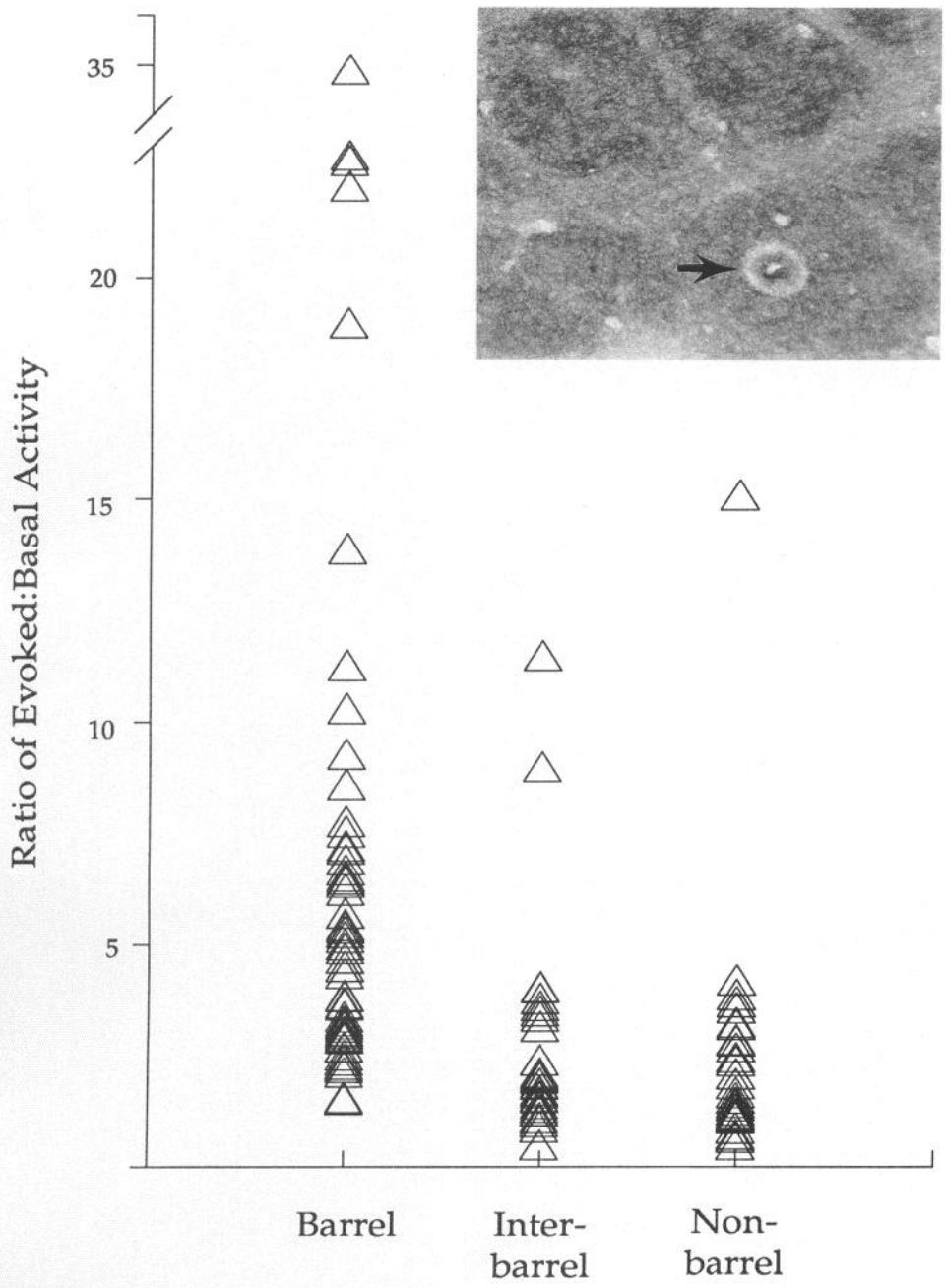

Figure 11. Ratio of evoked to basal activity in different regions in layer IV of the primary somatic sensory cortex in urethane-anesthetized adult rats. Each symbol represents the ratio of activity during sustained peripheral stimulation to the activity under basal conditions for a particular recording site (see Fig. 10, Table 4). Although the range of individual values was large for each group, the mean ratio was two to three times greater when the electrode was in barrels than when the recording site was in interbarrel regions or in nonbarrel S1 cortex (see Table 4). *Inset*, typical electrolytic lesion (*arrow*) used to identify each recording site (in this case the E5 barrel).

recordings from 13 animals, this stimulus increased the level of activity at barrel, interbarrel, and nonbarrel recording sites (Fig. 11, Table 4). The ratio of evoked to basal activity (as well as the absolute difference between these measurements) was greatest within barrels, less in interbarrel regions, and least, as expected, in the nonbarrel cortex (see Table 4).

Distribution of ^{3}H-2-DG accumulation

These electrophysiological observations are limited by the effects of anesthesia and uncertainty about the adequacy of the stimulus applied. We therefore examined the uptake of radiolabeled 2-DG in awake behaving animals. In autoradiograms

→

Figure 12. Differential uptake of ^{3}H-2-DG in the primary somatic sensory cortex of a representative juvenile rat. *A*, Montage of digitized autoradiograms from an awake behaving animal, showing the uptake of 2-DG in layer IV of S1 and the surrounding cortex. *B*, Color-coded map showing differential 2-DG uptake in and around S1 and its component parts; barrel borders were determined by SDH staining of the sections from which the autoradiograms were prepared. Scale bar, 2 mm.

Figure 13. Differential uptake of ^{3}H-2-DG in the primary somatic sensory cortex of a representative adult rat. *A*, Montage of digitized autoradiograms from an awake behaving animal, showing the uptake of 2-DG in layer IV of S1 and the surrounding cortex. *B*, Color-coded map showing differential 2-DG uptake in and around S1 and its component parts; barrel borders were determined by SDH staining of the sections from which the autoradiograms were prepared. Scale bar, 2 mm.

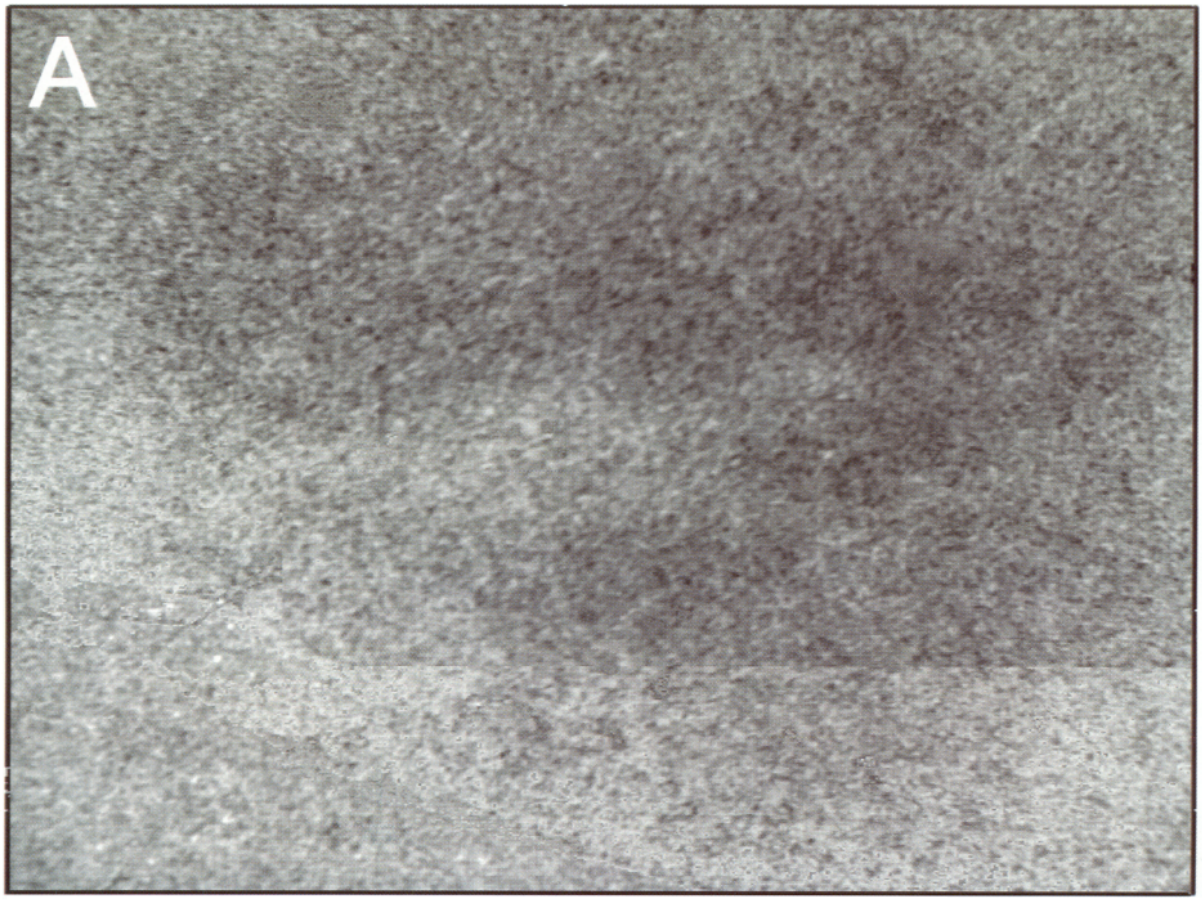
A

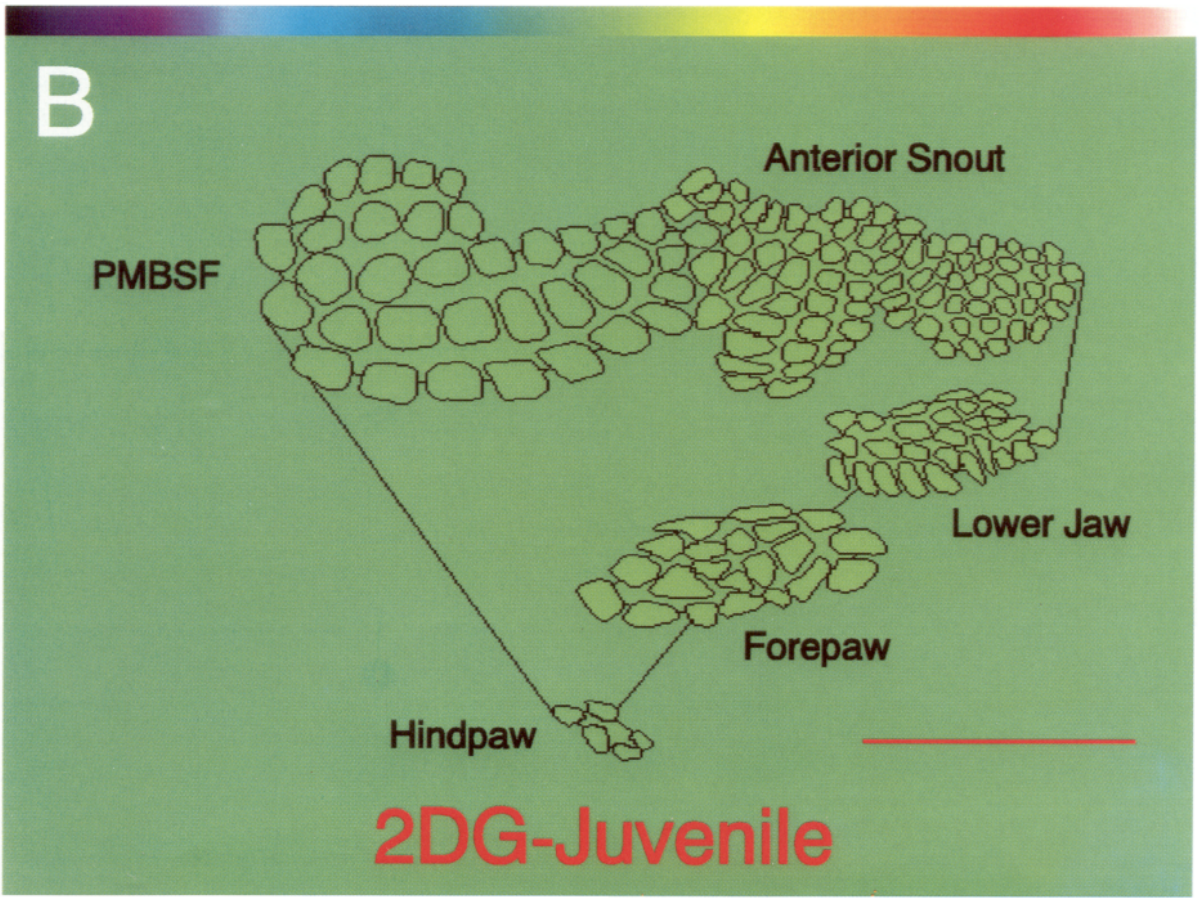
B
Anterior Snout
PMBSF
Lower Jaw
Forepaw
Hindpaw
2DG-Juvenile

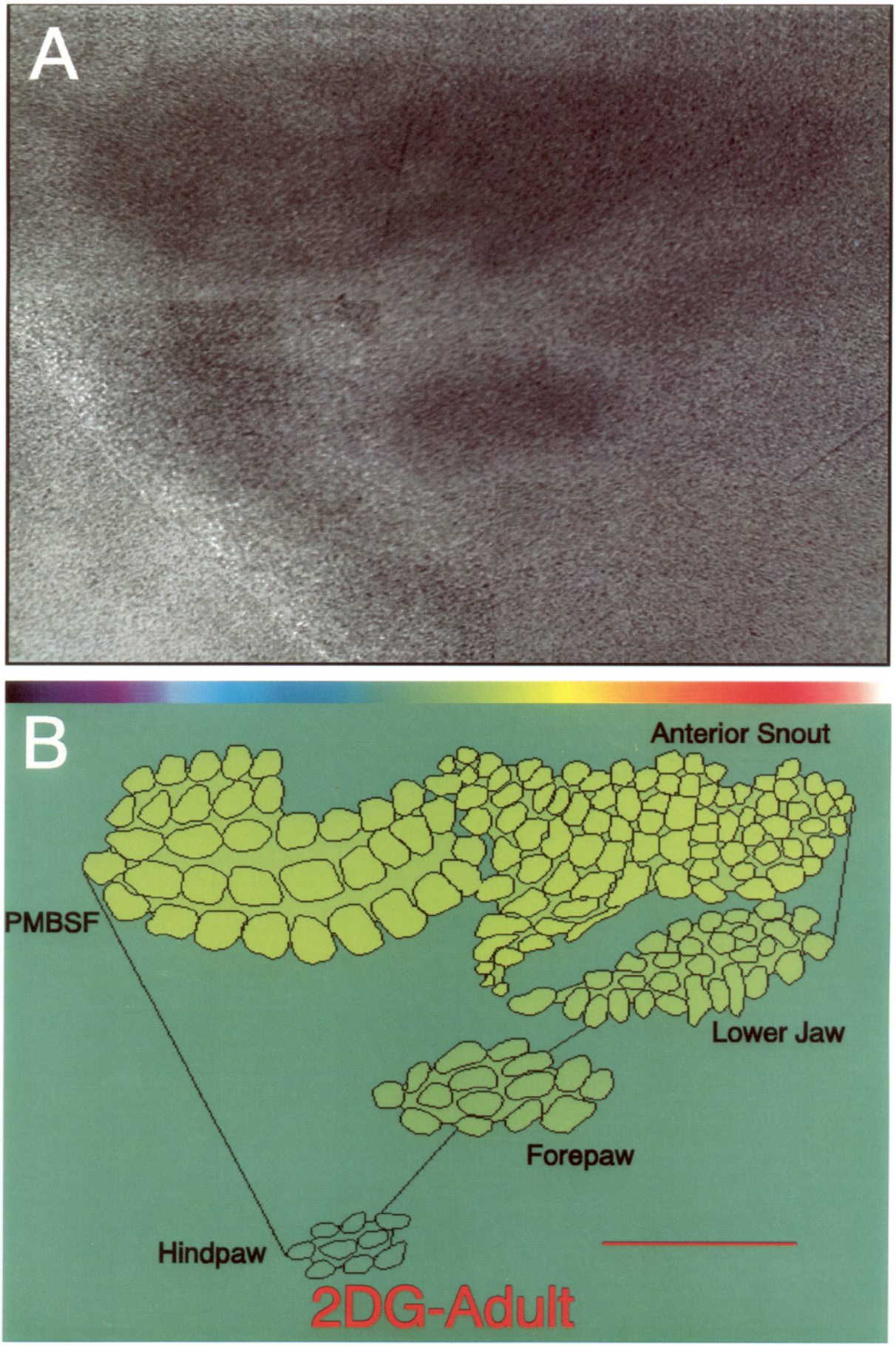
A
B
Anterior Snout
PMBSF
Lower Jaw
Forepaw
Hindpaw
2DG-Adult

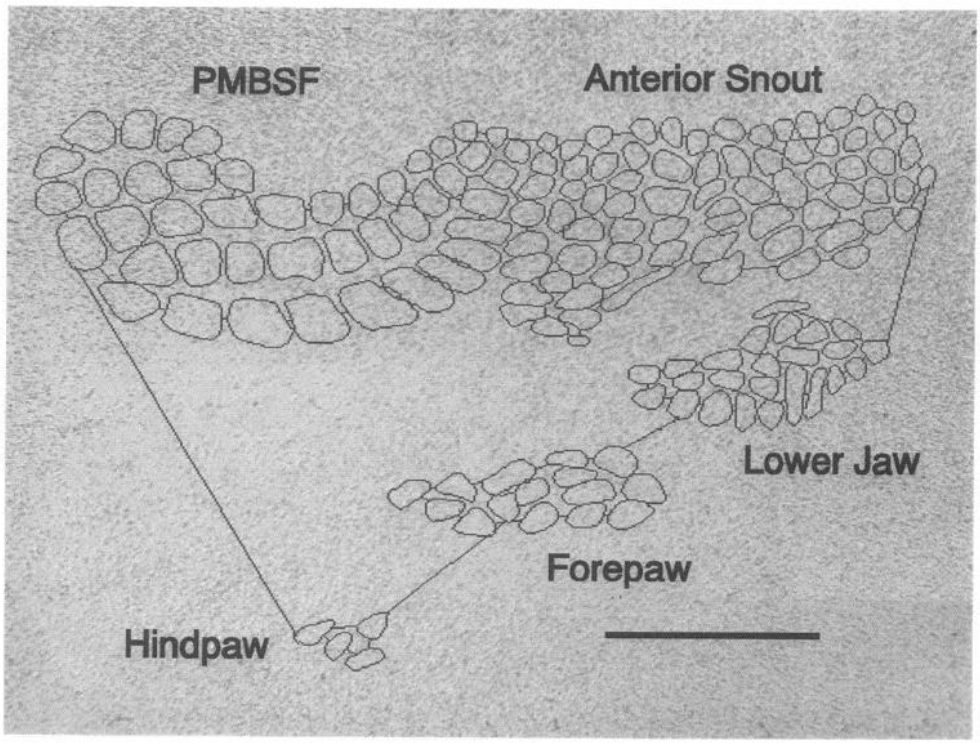

Figure 14. Suppression of differential 2-DG uptake in S1 by anesthesia. Montage of digitized autoradiograms from an adult rat anesthetized with urethane (1.5 gm/kg) throughout the 45 min period of 2-DG uptake. Autoradiograms from anesthetized animals showed much less overall 2-DG uptake compared to awake behaving animals (compare Fig. 13*A*). Scale bar, 2 mm.

of four juvenile hemispheres (four rats), S1 as a whole stood out from the surrounding cortex as a region of greater 2-DG accumulation (Fig. 12*A*). When the sections from which the autoradiograms had been prepared were counterstained with SDH to reveal barrels and barrel-like structures, it was apparent that the representations tended to accumulate more 2-DG than the surrounding cortex (Fig. 12*B*, Table 5).

An even more distinct pattern of 2-DG uptake was observed in autoradiograms of five adult hemispheres (four rats) (Table 5, Fig. 13). Barrels, wherever their location, accumulated more 2-DG than adjacent interbarrel, nonbarrel, or peri-S1 cortex. Overall, barrels in the head representation exhibited slightly greater 2-DG uptake than those in the paw regions.

These differences were not apparent in control experiments carried out on four adult animals anesthetized with either urethane or sodium pentobarbital during the period of 2-DG uptake (Fig. 14) (see above and Materials and Methods). This marked reduction in differential 2-DG uptake after anesthesia is consistent with the relatively small regional differences in basal electrical activity observed in unstimulated urethane-anesthetized animals (see above and Table 4).

The results of these observations on 2-DG accumulation in juvenile, adult, and anesthetized animals are consistent with our electrophysiological and metabolic analyses, confirming an ongoing pattern of differential cortical activity that matches the pattern of cortical growth.

Table 5. Relative levels of ^{3}H-2-DG uptake in the somatic sensory cortex of awake, behaving rats

Subjects	Number of hemispheres examined	Percentage differences (mean ± SEM) Barrel: interbarrel cortex	Barrel: nonbarrel S1 cortex	Barrel: peri-S1 cortex
Juvenile animals (1 week old)	4	1 ± 1	7 ± 1	8 ± 1
Adult animals (10–12 weeks old)	5	5 ± 1	13 ± 1	17 ± 1

Values were calculated as in Table 1.

Discussion

Many previous studies of the primary somatic sensory cortex have investigated the critical period for the formation of barrels (in rodents), or adult cortical plasticity (in rodents and primates) (reviewed in Killackey et al., 1990; Woolsey, 1990). The present work, in contrast, addresses activity-dependent modulation of cortical growth during postnatal maturation. Our studies thus begin after the critical period, at a time (1 week of age) when the cortical map in S1 in the rat is fully formed but much cortical growth—about a doubling of cortical area—still lies ahead (Riddle et al., 1992). This approach addresses a fundamental issue in neurobiology, namely, the effects of ongoing electrical activity on the amount of cortical circuitry ultimately devoted to different functions.

We have organized our evaluation of S1 along three general lines. First, we examined regional variations in metabolism by measuring the activity of mitochondrial enzymes and microvessel density. Second, we examined regional variations in metabolism that are more specifically related to electrical activity by measuring Na^+/K^+ ATPase staining. Finally, we examined electrical activity and 2-DG uptake in and around S1. In the aggregate, our results demonstrate systematic variations in average levels of neural activity across layer IV of this region of the developing rat brain. These differences correlate with regional variations in postnatal cortical growth, the more active

regions of S1 growing more than the less active ones (see Fig. 3 and Riddle et al., 1992). We therefore consider the possibility that differential cortical growth is modulated by levels of neural activity in the developing brain.

The relationship of metabolic and electrical activity

The indices we have used to examine S1 and its component parts reflect related but different aspects of neuronal activity.

SDH and CO histochemistry have long been used to visualize the S1 map in rodents (e.g., Dawson and Killackey, 1987; Wallace, 1987; Riddle et al., 1992). These mitochondrial enzymes are found primarily in the axon terminals (SDH) and dendrites (CO) of the neuropil (Killackey et al., 1976; Killackey and Belford, 1979; Wong-Riley, 1989). The representations of major body parts are apparent in S1 because of the relatively more intense staining of barrels and barrel-like structures (as well as larger patches like the trunk representation). Such differential staining suggests that ongoing metabolic activity within S1 is heterogeneous. In adult animals at least, the activity of these and other enzymes responsible for energy production in the brain has been taken to reflect the tight coupling of oxidative metabolism and neuronal activity (e.g., Sokoloff, 1977, 1978, 1979, 1981; Wong-Riley, 1989). The differential distribution of mitochondrial enzymes is paralleled by the distribution of microvessels in S1. This finding accords with other evidence that the vascularization of the cortex varies from region to region, apparently reflecting the chronic metabolic demand of functionally different areas (Campbell, 1939; Patel, 1983; Weibel, 1984; Borowsky and Collins, 1989; Zheng et al., 1991).

The pattern of Na^+/K^+ ATPase staining also implies systematic variations in average levels of neural activity across this part of the cortex. Sodium/potassium ATPase is located primarily in neuropil (Lewin and Hess, 1964; Stahl and Broderson, 1976a,b; Hevner et al., 1992). This enzyme, which consumes about half the ATP produced in the brain, is a particularly good index of neuronal activity since it maintains the ion gradients required for signaling (Mata et al., 1980; Erecinska and Silver, 1989). Thus, this result addresses a problem inherent in the use of metabolic markers to evaluate electrical activity in the maturing brain, namely, the energy requirements of growth per se. The distribution of ATPase indicates that the differential metabolism apparent with other markers in the juvenile somatic sensory cortex reflects, at least in large part, regional variations of neural activity. The persistence of differential metabolism across the adult S1 after growth has ceased accords with this interpretation.

We nonetheless deemed it important to evaluate electrical activity directly. Although neuronal responses to whisker stimulation have been assessed in both anesthetized and awake rodents (Armstrong-James, 1975; Welker, 1976; Simons, 1978, 1985; Simons and Woolsey, 1979; Simons et al., 1992), these observations have focused on the receptive field properties of single units rather than on the overall levels of electrical activity across S1. Our electrophysiological recordings showed that neurons in barrels of the PMBSF are more active in response to generalized mechanosensory stimulation of the face than neurons in interbarrel or adjacent nonbarrel regions. These experiments under anesthesia, however, may not reflect normal patterns of sensory activity. We therefore used labeled 2-DG to study the ongoing activity of S1 in awake behaving animals. This marker is taken up primarily by active presynaptic terminals (Sharp, 1976; Mata et al., 1980). In agreement with the other indices examined, densitometric analysis showed greater 2-DG uptake in barrels than in interbarrel or nonbarrel cortex, greater uptake in the barrels of the head representation than in the representations of the paws, and greater uptake in S1 than in the surrounding cortex. Taken together, these results provide strong evidence for systematic regional differences in neuronal activity across this part of the mammalian neocortex.

The significance of greater neural activity in barrels

Perhaps the most salient feature of the rat somatic sensory cortex is the presence of barrels and barrel-like structures. Barrels were initially described in relation to, and have long been associated with, the mystacial vibrissae of rodents and other mammals (Woolsey and Van der Loos, 1970; Woolsey et al., 1975). It has become apparent, however, that structures in layer IV similar to those in the PMBSF occur throughout the primary somatic sensory cortex and indeed elsewhere in the cortex (Dawson and Killackey, 1987; Riddle et al., 1992). The barrel-like structures in the paw representations are associated with the digital and palmar pads (Dawson and Killackey, 1987); therefore, it seems likely that these entities always represent special sensors. We have found no systematic difference in the functional characteristics of the barrels related to mystacial vibrissae and other barrel-like structures throughout S1. These layer IV modules are universally characterized by increased mitochondrial enzyme activity, increased capillary density, increased Na^+/K^+ ATPase activity, and increased electrical activity relative to the immediately surrounding cortex.

A trivial explanation of these regional variations might be that they simply reflect an uneven distribution of cell bodies and neuropil that corresponds precisely to the arrangement of barrels or other modular elements. Although there are, of course, cytoarchitectonic differences associated with barrels (this is how barrels were first noticed), these features seem unlikely to explain the metabolic and electrical characteristics of these structures. First, differences in cell body and synaptic (or neuropil) density across barrel and interbarrel regions do not always coincide with barrel boundaries (Patel-Vaidya, 1985). Second, other cytoarchitectonic differences among barrels do not correspond to the metabolic and electrical patterns we describe. For example, anterior snout barrel centers are relatively poor in cell bodies, whereas PMBSF barrel centers are rich in cell somata (Welker and Woolsey, 1974; Patel-Vaidya, 1985). Nonetheless, barrels throughout the head representation are characterized by high levels of metabolic and electrical activity. The structural feature that best correlates with barrels and barrel-like structures is the presence of thalamic afferents from the ventrobasal complex, which are presumably the proximal source of their greater electrical activity. Third, the formation of barrels can apparently be elicited in any cortical region by the functional consequences of innervation by these thalamic afferents (Schlagger and O'Leary, 1991).

We have recently argued that the major significance of modules, whether in the somatic sensory cortex or elsewhere, is that they represent foci of coherent neural activity (Purves et al., 1992). Evidently, when regional levels of electrical activity in S1 contrast sufficiently, modules become apparent anatomically by one or more of the methods we have used here. In short, we propose that the pattern of barrel and barrel-like structures in S1 is, among other things, a manifestation of regional differences in average levels of neural activity, in both development and maturity.

Neural activity and cortical growth

The correlation of regional differences in neural activity with regional differences in postnatal cortical growth is striking (see Fig. 3). Barrels and barrel-like structures have the highest levels of metabolic and electrical activity within S1 and grow most during postnatal maturation. Furthermore, the barrels in somatic representations in which there is greatest metabolic activity grow to a greater extent than those in less active representations. Finally, S1 as a whole grows more than the neocortex generally, and is revealed in these studies as being, on average, metabolically and electrically more active than the surrounding cortex.

It should be noted that several recent reports suggest that electrical activity plays little role in the initial formation of barrels and barrel-like structures in S1 or its subcortical relays. Thus, silencing the neonatal cortex (or the corresponding peripheral sensors) for a few days after birth with TTX or by other means does not interfere with the appearance of apparently normal cortical barrels, and the related entities in the thalamus and brainstem (Bauer et al., 1992; Chiaia et al., 1992; Henderson et al., 1992; Schlagger and O'Leary, 1992). Evidently, the initial formation of such entities is not strongly influenced by function, unlike the formation of modular patterns in the visual system (e.g., Shatz, 1990). These differences between the somatic sensory and the visual system, and their relationship to the present work, must eventually be explained.

The overall growth of S1 (or any other region of the brain) is certainly not *caused* by neural activity; neural growth is a complex phenomenon to which many factors contribute (reviewed in Purves and Lichtman, 1985; Purves, 1988, 1993). Rather, we suggest that brain growth is *modulated* by regional differences in activity, which thus regulate the amount of neuropil devoted to various functional roles in the mature brain. Such activity-modulated cortical growth could explain how the effects of experience can be permanently encoded in the developing nervous system.

References

Armstrong-James M (1975) The functional status and columnar organization of single cells responding to cutaneous stimulation in neonatal rat somatosensory cortex S1. J Physiol (Lond) 246:501–538.

Armstrong-James M, Fox K (1983) Similarities in unitary cortical activity between slow-wave sleep and light urethane anesthesia in the rat. J Physiol (Lond) 346:55P.

Armstrong-James M, Caan AW, Fox K (1985) Threshold effects of *N*-methyl D-aspartate (NMDA) and 2-amino 5-phosphonovaleric acid (2APV) on the spontaneous activity of neocortical single neurones in the urethane anesthetized rat. Exp Brain Res 60:209–213.

Bauer WR, Chiaia NL, Fish SE, Figley BA, Eck M, Bennett-Clarke CA, Rhoades RW (1992) Effects of postnatal blockade of cortical activity upon the development and plasticity of vibrissae-related patterns in the somatosensory cortex of rat and hamster. Soc Neurosci Abstr 18: 620.

Borowsky IW, Collins RC (1989) Metabolic anatomy of brain: a comparison of regional capillary density, glucose metabolism, and enzyme activities. J Comp Neurol 288:401–413.

Campbell ACP (1939) Variation in vascularity and oxidase content in different regions of the brain of the cat. Arch Neurol Psychiatry 41:223–242.

Chapin JK, Lin C-S (1984) Mapping the body representation in the SI cortex of anesthetized and awake rats. J Comp Neurol 229:199–213.

Chiaia NL, Fish SE, Bauer WR, Bennett-Clarke CA, Rhoades RW (1992) Postnatal blockade of cortical activity by tetrodotoxin does not disrupt the formation of vibrissa-related patterns in the cat's somatosensory cortex. Dev Brain Res 66:244–250.

Dawson DR, Killackey HP (1987) The organization and mutability of the forepaw and hindpaw representations in the somatosensory cortex of neonatal rat. J Comp Neurol 256:246–256.

Erecinska M, Silver IA (1989) ATP and brain function. J Cereb Blood Flow Metab 9:2–19.

Fox K, Armstrong-James M (1986) The role of the anterior intralaminar nuclei and *N*-methyl D-aspartate receptors in the generation of spontaneous bursts in rat neocortical neurones. Exp Brain Res 63: 505–518.

Goodman CS, Shatz CJ (1993) Developmental mechanisms that generate precise patterns of neuronal connectivity. Neuron 10:77–98.

Henderson TA, Woolsey TA, Jacquin MF (1992) Infraorbital nerve blockade from birth does not disrupt central trigeminal pattern formation in the rat. Dev Brain Res 66:146–152.

Hevner RF, Duff RS, Wong-Riley MTT (1992) Coordination of ATP production and consumption in brain: parallel regulation of cytochrome oxidase and Na^+, K^+-ATPase. Neurosci Lett 138:188–192.

Killackey HP, Belford GR (1979) The formation of afferent patterns in the somatic sensory cortex of the neonatal rat. J Comp Neurol 183: 285–304.

Killackey HP, Belford G, Ryugo R, Ryugo DK (1976) Anomalous organization of thalamocortical projections consequent to vibrissae removal in the newborn rat and mouse. Brain Res 104:309–315.

Killackey HP, Jacquin MF, Rhoades RW (1990) Development of somatosensory structures. In: Development of sensory systems in mammals (Coleman JR, ed), pp 403–429. New York: Wiley.

Kugler P (1982) Quantitative dehydrogenase histochemistry with exogenous electron carriers (PMS, MPMS, MB). Histochemistry 75:99–112.

Kugler P, Vogel S, Gehm M (1988) Quantitative succinate dehydrogenase histochemistry in the hippocampus of aged rats. Histochemistry 88:299–307.

Lewin E, Hess HH (1964) Intralaminar distribution of Na^+-K^+ adenosine triphosphatase in rat cortex. J Neurochem 11:473–481.

Mata M, Fink DJ, Gainer H, Smith CB, Davidsen L, Savaki H, Schwartz WJ, Sokoloff L (1980) Activity-dependent energy metabolism in rat posterior pituitary primarily reflects sodium pump activity. J Neurochem 34:213–215.

Patel U (1983) Non-random distribution of blood vessels in the posterior region of the rat somatosensory cortex. Brain Res 289:65–70.

Patel-Vaidya U (1985) Ultrastructural organization of posterior and anterior barrels in the somatosensory cortex of rat. J Neurosci Res 14:357–371.

Purves D (1988) Body and brain: a trophic theory of neural connections. Cambridge, MA: Harvard UP.

Purves D (1993) Neural activity and the growth of the brain. Cambridge: Cambridge UP.

Purves D, Lichtman J (1985) Principles of neural development. Sunderland, MA: Sinauer.

Purves D, Riddle D, LaMantia A-S (1992) Iterated patterns of brain circuitry (or how the cortex gets its spots). Trends Neurosci 15:362–368.

Richardson K, Rosen SPR (1971) Incorporation of lysine into rat brain: a diurnal rhythmicity. Nature 223:182–184.

Riddle D, Richards A, Zsuppan F, Purves D (1992) Growth of the rat somatic sensory cortex and its constituent parts during postnatal development. J Neurosci 12:3509–3524.

Schlagger BL, O'Leary DDM (1991) Potential of visual cortex to develop an array of functional units unique to somatosensory cortex. Science 252:1556–1560.

Schlagger BL, O'Leary DDM (1992) An activity dependent component of plasticity in the developing rat neocortex. Soc Neurosci Abstr 18: 57.

Sharp FR (1976) Relative cerebral glucose uptake of neuronal perikarya and neuropil determined with 2-deoxyglucose in resting and swimming rat. Brain Res 110:127–139.

Shatz CJ (1990) Impulse activity and the patterning of connections during CNS development. Neuron 5:745–756.

Simons DJ (1978) Response properties of vibrissa units in rat S1 somatic sensory neocortex. J Neurophysiol 41:798–820.

Simons DJ (1985) Temporal and spatial integration in the rat S1 vibrissa cortex. J Neurophysiol 54:615–635.

Simons DJ, Woolsey TA (1979) Functional organization in mouse barrel cortex. Brain Res 165:327–332.

Simons DJ, Carvell GE, Hershey AE, Bryant DP (1992) Responses of barrel cortex neurons in awake rats and effects of urethane anesthesia. Exp Brain Res 91:259–272.

Sokoloff L (1977) Relation between physiological function and energy metabolism in the central nervous system. J Neurochem 29:13–26.
Sokoloff L (1978) Metabolic probes of central nervous system activity in experimental animals and man. Sunderland, MA: Sinauer.
Sokoloff L (1979) Mapping of local cerebral functional activity by measurement of local cerebral glucose utilization with (^{14}C) deoxyglucose. Brain 102:653–668.
Sokoloff L (1981) Localization of functional activity in the central nervous system by measurement of glucose utilization with radioactive deoxyglucose. J Cereb Blood Flow Metab 1:7–36.
Stahl WL, Broderson SH (1976a) Histochemical localization of potassium-stimulated *p*-nitrophenyl phosphatase activity in the somatosensory cortex of the rat. J Histochem Cytochem 24:731–739.
Stahl WL, Broderson SH (1976b) Localization of Na^+/K^+ ATPase in brain. Fed Proc 35:1260–1265.
Wallace MN (1987) Histochemical demonstration of sensory maps in the rat and mouse cerebral cortex. Brain Res 418:178–182.
Weibel ER (1984) The pathway for oxygen: structure and function in the mammalian respiratory system. Cambridge, MA: Harvard UP.
Welker C (1976) Receptive fields of barrels in the somatosensory neocortex of the rat. J Comp Neurol 166:173–190.
Welker C, Woolsey TA (1974) Structure of layer IV in the somatosensory neocortex of the rat: description and comparison with the mouse. J Comp Neurol 158:437–454.
Wiesel TN, Hubel DH (1963) Single cell responses in striate cortex of kittens deprived of vision in one eye. J Neurophysiol 26:1003–1017.
Wong-Riley MTT (1979) Changes in the visual system of monocularly sutured or enucleated cats demonstrable with cytochrome oxidase histochemistry. Brain Res 171:11–28.
Wong-Riley MTT (1989) Cytochrome oxidase: an endogenous metabolic marker for neuronal activity. Trends Neurosci 12:94–101.
Woolsey TA (1990) Peripheral alterations and somatosensory development. In: Development of sensory systems in mammals (Coleman JR, ed), pp 461–516. New York: Wiley.
Woolsey TA, Van der Loos H (1970) The structural organization of layer IV in the somatic sensory region (S1) of mouse cerebral cortex. Brain Res 17:205–242.
Woolsey TA, Dierker ML, Wann DF (1975) Mouse SmI cortex: qualitative and quantitative classification of Golgi-impregnated barrel neurons. Proc Natl Acad Sci USA 72:2165–2169.
Zheng D, LaMantia AS, Purves D (1991) Specialized vascularization of the primate visual cortex. J Neurosci 11:2622–2629.